

1 **Bringing Ancient Loess Critical Zones into A New Era of**  
2 **Sustainable Development Goals**

3 Xiaoxu Jia<sup>1,2,3</sup>, Ping Zhu<sup>1,2</sup>, Xiaorong Wei<sup>3\*</sup>, Yuanjun Zhu<sup>3</sup>, Mingbin Huang<sup>3</sup>, Wei Hu<sup>4</sup>,  
4 Yunqiang Wang<sup>5</sup>, Tuvia Turkeltaub<sup>6</sup>, Andrew Binley<sup>7</sup>, Robert Horton<sup>8</sup>, Ming'an Shao<sup>1,2,3\*</sup>

5 <sup>1</sup>Key Laboratory of Ecosystems Network Observation and Modeling, Institute of Geographic  
6 Sciences and Natural Resources Research, Chinese Academy of Sciences, Beijing 100101,  
7 China

8 <sup>2</sup>College of Resources and Environment, University of Chinese Academy of Sciences, Beijing  
9 100190, China

10 <sup>3</sup>State Key Laboratory of Soil Erosion and Dryland Farming on the Loess Plateau, Northwest  
11 A&F University, Yangling, Shaanxi 712100, China

12 <sup>4</sup>New Zealand Inst Plant & Food Res Ltd, Private Bag 4704, Christchurch 8140, New Zealand

13 <sup>5</sup>State Key Laboratory of Loess and Quaternary Geology, Institute of Earth Environment, Chinese  
14 Academy of Sciences, Xi'an, Shaanxi 710061, China

15 <sup>6</sup>Zuckerberg Institute for Water Research, Blaustein Institutes for Desert Research, Ben-Gurion  
16 University of the Negev, Sede Boqer Campus 8499000, Israel

17 <sup>7</sup>Lancaster Environment Centre, Lancaster University, Bailrigg, Lancaster, LA1 4YQ, UK

18 <sup>8</sup>Iowa State University, Ames, Iowa 50011, USA

19

20 \*Correspondences: Xiaorong Wei ([xrwei78@163.com](mailto:xrwei78@163.com)), State Key Laboratory of Soil Erosion  
21 and Dryland Farming on the Loess Plateau, Northwest A&F University, Yangling, Shaanxi  
22 712100, China; Ming'an Shao ([shaoma@igsnr.ac.cn](mailto:shaoma@igsnr.ac.cn)), Key Laboratory of Ecosystems Network  
23 Observation and Modeling, Institute of Geographic Sciences and Natural Resources Research,  
24 Chinese Academy of Sciences, Beijing 100101, China

25

26

27

28

29

30

31

32 **Abstract:** Critical Zone Observatories (CZOs) have been established initially in natural  
33 environments to monitor CZ processes. A new generation of CZOs has been extended  
34 to human-modified landscapes to address the impacts of climate change and human-  
35 caused actions such as erosion, droughts, floods, and water resource pollution. This  
36 review focuses on numerous plot, field, and regional scale studies conducted in the CZO  
37 facilities distributed across the China Loess Plateau (CLP). The CLP CZO features the  
38 world's largest and deepest loess deposits, highly disturbed by human activities, and  
39 consists of a longitudinal series of monitoring sites. This observation system consists  
40 of plot, slope, watershed, and regional observatories and is promoted by large-scale  
41 comprehensive experiments to achieve multiscale observations. Deep soil boreholes,  
42 hydro-geophysical tools, multiple tracers-based techniques, proximal and remote  
43 sensing techniques, and automatic monitoring equipment are implemented to monitor  
44 CZ processes. Observation and modeling of critical hydrological and biogeochemical  
45 processes (e.g., water, nutrients, carbon, and microbial activities) in land surface and  
46 deep loess deposits across CLP CZOs have unveiled crucial insights into human-  
47 environment interactions and sustainability challenges. Large-scale ecological efforts  
48 such as revegetation and engineering such as check dam construction have effectively  
49 mitigated flood and soil erosion while enhancing deep soil carbon sequestration.  
50 However, these interventions can yield both benefits and drawbacks, impacting deep  
51 soil water, groundwater recharge, and agricultural production. Converting arable  
52 cropland to orchards for increased income has raised nitrate accumulation in the deep  
53 vadose zone, posing a risk of groundwater pollution. These findings, combined with the  
54 CZ data, have identified knowledge exchange opportunities to unravel diverse factors  
55 within the relations of agriculture, ecosystem, and environment. These could directly  
56 improve local livelihoods and eco-environmental conditions by optimizing land use and  
57 management practices, increasing water use efficiency, and reducing fertilizer  
58 application. These efforts contribute toward Sustainable Development Goals (SDGs)  
59 and environmental policies. Overall, studies within the CLP have provided significant  
60 scientific advancements and guidance on managing CZ processes and services with  
61 regional SDGs, that may be transferable to other highly disturbed regions of the world.

62 **Keywords:** Loess critical zone (CZ); Ecohydrological processes; Biogeochemical  
63 processes; CZ services; Human activities

## 64 **1. Introduction**

65 The Critical Zone (CZ) is the thin outer layer of our planet, extending from the top  
66 of the vegetation canopy to the bottom of groundwater aquifers in terrestrial  
67 environments and encompasses the atmosphere, biosphere, pedosphere, hydrosphere,  
68 and lithosphere (National Research Council, 2001). CZ science explores how  
69 landscapes evolve from below the Earth's surface to the top of vegetation, supporting  
70 all terrestrial life on Earth (Naylor et al., 2023). CZ science is driving a new  
71 understanding of the links that connect geomorphology, hydrology, climate, ecosystems,  
72 and geology. Critical Zone Observatories (CZOs) have been established initially in  
73 "natural" environments to monitor CZ processes (Chorover et al., 2007). However, a  
74 transition has occurred where the legacy of natural processes has been affected to  
75 various extents by land use and other direct human interactions with ecosystems (Guo  
76 and Lin, 2016). The equilibrium of the natural environment is increasingly disrupted.  
77 Thus, monitoring CZ processes at CZOs has been extended to human-modified  
78 landscapes that dominant our world (Minor et al., 2020; Naylor et al., 2023), showing  
79 an evolution from an initial to a new generation of CZOs. The new generation CZO  
80 programmes aim to develop a deeper understanding of the impacts of human  
81 modification on landscapes.

82 Loess deposits are CZs that host over 321 million people and are characterized by  
83 high disturbances, productive and dynamic ecosystems, ongoing environmental change,  
84 and significant values to society. Loess deposits are widely distributed in the mid-  
85 latitude arid to semi-arid regions of both the northern and southern hemispheres (Fig.  
86 1a), at altitudes ranging from several meters near the coasts (such as in Argentina and  
87 New Zealand) to 5300 m north of the Kunlun Mountains of China (Li et al., 2020).  
88 Loess deposits are of variable thickness, from a few meters to >300 m worldwide. The  
89 thickest (generally between 10 and 300 m thick with a maximum thickness of 500 m)  
90 and most continuous loess deposits worldwide are located on the Chinese Loess Plateau

91 (CLP; [Zhu et al., 2018](#)). The thicknesses of loess in Siberia and Central Asia are usually  
92 <200 m. The thicknesses of loess in Europe and North America typically do not exceed  
93 20 m. Still, they can be close to 100 m in the Lower Danube River, the Palouse Region  
94 of NW USA, Nebraska, and Alaskan regions ([Li et al., 2020](#)). Thick loess deposits  
95 preserve a record of a wide variety of recent and past environments, such as  
96 paleoclimatic and paleomagnetic variations at various time scales ([Kemp, 2001](#); [Liu et al., 2015](#); [Sun et al., 2021](#)). The areas covered by thick loess and similar deposits  
97 constitute important and unique CZs on Earth, which are quite different from CZs  
98 developed on other lithologies (e.g., karst regions, arctic regions or coastal margins)  
99 regarding hydrological and biogeochemical processes. Because of the extensive  
100 distribution of loess deposits and typically intensive anthropogenic disturbances, loess  
101 regions should be considered an important geographic focus for CZ science. Loess-  
102 based observations are also critical for understanding systems influenced by eolian,  
103 pedogenic or drought, agricultural practices, and vegetation restoration. Over the past  
104 two centuries, there have been two main themes of loess study in the world, i.e., the  
105 origin of the loess deposit and the linkage between climate and loess ([Smalley et al.,](#)  
106 [2001](#)).  
107

108 Loess CZs are known to have supported prehistorical agricultural civilizations.  
109 Generally, loess has a homogenous and porous structure and consists primarily of quartz  
110 and felspar particles. Loess soils are among the most fertile in the world, principally  
111 because the abundance of silt particles ensures a good supply of plant-available water,  
112 good soil aeration, extensive penetration by plant roots, and easy cultivation and  
113 seedbed preparation ([Catt, 2001](#)). The inherent physical and chemical fertility of loess  
114 soils had an important prehistorical role in developing early civilizations, such as those  
115 of China and Europe. The fertile top-soils of loess landscapes have been extensively  
116 utilized in agricultural practices since the Neolithic period, starting 7000 years ago  
117 ([Whittle and Whittle, 1996](#); [Bellwood, 2005](#)). The agricultural use of the loess lowlands  
118 has generally been highly specialized from the past to the present. For example, Chinese  
119 culture originated on the CLP and adjacent areas of the North China Plain  
120 approximately 7000 years ago ([Liu, 2004](#); [Rosen, 2008](#)). Therefore, thousands of years

121 of agricultural practices may have significantly impacted on the landscapes and  
122 environments in the loess CZs.

123 Although loess is fertile, it is also extremely susceptible to both wind and water  
124 erosion since loess from aeolian deposits generally has very high porosity, loose particle  
125 packing, and consequently low bulk density (Feng et al., 2021). Furthermore, these  
126 deposits often contain little clay, leading to organic matter loss under arable cultivation.  
127 Water shortage and low vegetation cover are also common problems in loess areas in  
128 arid and semi-arid climatic regions, which increase the difficulty of ecological  
129 environment protection and restoration in these areas. Water resources in water-stressed  
130 loess areas are primarily provided by precipitation, and excessive use of soil water by  
131 vegetation, particularly establishing anthropogenic vegetation, can potentially lead to a  
132 severe imbalance between water supply and demand due to limited rainwater resources  
133 (Zhang et al., 2018a; Li et al., 2023a, b). Reduction in local water availability can, in  
134 turn, threaten the health and services of restored ecosystems, as well as human  
135 agricultural and industrial activities, particularly in densely populated and water-limited  
136 arid and semi-arid regions. All these problems widely exist in loess areas around the  
137 world, such as England (Boardman and Hazelden, 1986), Belgium (Evrard et al., 2008),  
138 USA (Hanson and Simon, 2001; Bettis et al., 2003), Iran (Doulabian et al., 2021;  
139 Sadeghi et al., 2021), France (Delmas et al., 2012; Kervroëdan et al., 2019) and China  
140 (Fu et al., 2017; Shao et al., 2018). Nevertheless, loess areas are eco-environmentally  
141 vulnerable in the world due to serious soil erosion, water shortage, low vegetation cover,  
142 and frequent and intensive human disturbances (Dotterweich, 2013; Fu et al., 2017).  
143 Research is needed urgently to address these problems and avoid permanently  
144 degrading CZ function.

145 Soil and water are the most vital natural resources in the CZ, as they directly  
146 impact food security, human health, and CZ function (Lin, 2010; Vereecken et al., 2015;  
147 Banwart et al., 2019). Soil and water processes within the CZ, such as soil formation,  
148 hydrologic partitioning, runoff generation, carbon (C) sequestration, nutrient and  
149 biogeochemical cycling, support and/or control of the supplies and benefits that the CZ  
150 produces through these processes for humans and the surrounding environment (Zhu et

151 [al., 2015a; Zhang et al., 2019](#)) (Fig. 2a). Previous reports on loess CZs emphasize that  
152 soil and water are critical to numerous CZ services, such as *provisioning services* (e.g.,  
153 water, food, and other resources supply), *regulating services* (e.g., water quality, flood  
154 regulation, and climate regulation), and *supporting services* (e.g., soil conservation, soil  
155 formation, C sequestration, and nutrient cycle). These CZ services, in turn, directly  
156 contribute to various Sustainable Development Goals (SDGs) ([Field et al., 2015;](#)  
157 [Richardson and Kumar, 2017; Lal et al., 2021](#)) (Fig. 2b). The CLP CZ has the thickest  
158 and most continuous loess deposits in the world. Long-term intensive anthropogenic  
159 disturbances (e.g., farming and large-scale ecological restoration) have greatly altered  
160 surface landscape properties and critical soil and water processes in the deeper  
161 subsurface of the CLP and, consequently, the CZ functions. The depth of measurements  
162 is thus important for loess CZ research, which is quite different from other CZs covered  
163 by thin soils. Exploring the impacts of anthropogenic activities at the land surface on  
164 deeper subsurface hydrological properties and biogeochemical processes with  
165 multidisciplinary collaborations and multiple analytical techniques can advance a  
166 comprehensive understanding of human-environment interactions.

167 Historically, the increasing demand for cultivated land and grain production has  
168 led to the destruction of natural vegetation and subsequent worsening of soil erosion on  
169 the CLP, which in turn, has led to an increase in floods in the Yellow River (YR) Basin  
170 ([Chen et al., 2012; Wang et al., 2021a](#)). However, various positive measures, such as  
171 slope cropland abandonment, afforestation, and cropland-to-orchard transition, have  
172 been implemented to improve the eco-environment and farmers income via increasing  
173 vegetation cover, reducing soil erosion, decreasing flood disasters, and enhancing C  
174 sequestration in the CLP in recent decades. Nonetheless, emerging problems such as  
175 food insecurity, water shortage, and severe residual nitrate pollution, hinder the  
176 sustainable development of the eco-environment in the CLP. These problems are closely  
177 associated with surface and subsurface processes interacting under different human  
178 activities, and economic-environmental trade-offs that occur in the loess CZ ([Gao et al.,](#)  
179 [2021a; Wang et al., 2021a](#)). Thus, the key issue to be addressed within loess CZOs is  
180 understanding critical soil and water processes in both surface and deeper subsurface

181 and how these processes respond to natural and anthropogenic changes (Fig. 2a).  
182 Addressing these issues will have great significance on the judicious management of  
183 soil and water resources within CZs, and is important for supporting regional SDGs.  
184 Specific scientific questions for loess CZs are:

- 185 ■ Can surface soil erosion be controlled or alleviated?
- 186 ■ Does a large-scale ecological program affect local food security?
- 187 ■ Does large-scale vegetation restoration exacerbate water scarcity?
- 188 ■ Can desiccated deep soils be hydrologically recharged and restored?
- 189 ■ Does precipitation recharge groundwater in thick loess CZs?
- 190 ■ What are the ecohydrological functions of weathered bedrock?
- 191 ■ Do agricultural practices impact groundwater quality?
- 192 ■ Does deep loess soil sequester C from the atmosphere?

193 In this paper, we first examine the CLP as a typical example to describe a loess  
194 CZ's basic hydrogeomorphic features and provide a framework for watershed  
195 observatories and best-available datasets. We then discuss critical soil and water process  
196 responses to natural and anthropogenic changes occurring on a loess CZ. Finally, we  
197 summarize new insights that can benefit the sustainable development of loess CZ's eco-  
198 environmental and social needs. This study provides a roadmap to advancing CZ  
199 science and inform stakeholders.

## 200 **2. Loess CZ Observatories and Basic Observations**

201 The development of CZ science has aroused global interest resulting in more than  
202 100 CZOs located in 29 countries being established since 2007 to form a global network  
203 of observatories (Lin et al., 2011; Niu et al., 2014; Giardino and Houser, 2015; Guo and  
204 Lin, 2016) (Fig. 1a). However, there are only a few CZOs in the loess regions. The lack  
205 of knowledge on critical soil and water processes in response to high disturbances  
206 inhibits the achievement of regional SDGs in loess-covered regions of the world. In  
207 China, scientists, engineers, and managers attach great importance to the loess CZs.  
208 There are several observation stations for soil, water, and vegetation processes on the  
209 CLP, which constitute the loess CZO's network (Fig. 1b). Within the loess CZO's

210 network, several representative watersheds are chosen as the core sites for soil-water-  
211 ecosystem research (Fig. 1b and Table S1), as they cover distinct gradients in the  
212 geomorphologic landscape, climate, and human activities across the CLP. Thus,  
213 compared to other CZOs around the world, the uniqueness of the setup of the CLP CZO  
214 is that it consists of a longitudinal series of monitoring sites rather than a single  
215 observatory sub-watershed (Jia et al., 2020).

216 Notably, there are several other CZOs located in the loess-covered regions, such  
217 as the Intensively Managed Landscapes CZO (IML-CZO) in the US Midwest (Fig. 1a).  
218 The IML-CZO's network is composed of three highly characterized, well instrumented,  
219 and representative watersheds (i.e., Clear Creek, Iowa; Upper Sangamon River, Illinois;  
220 and Minnesota River, Minnesota). In the Clear Creek watershed, the loess deposit is  
221 about 15 m thick and covers till and clayey paleosols. In comparison, the Upper  
222 Sangamon and Minnesota River basins are mantled with thin loess deposits that  
223 transition vertically to unweathered fine-grained glacial till within 5 m of the land  
224 surface (Bettis et al., 2003; Wilson et al., 2018). The IML-CZO focuses on the US  
225 Midwest, one of the world's most intensively managed landscapes. It provides an  
226 understanding of how land-use changes affect the long-term resilience of the CZ,  
227 similar to the loess CZOs in China.

228 Generally, the soil and water processes of the Chinese loess CZOs are  
229 characterized by multiscale monitoring approaches (Fig. 3). At the plot or slope scale,  
230 techniques such as single automatic sensors, neutron probes, borehole drilling, and  
231 laboratory analyses are employed. Borehole drilling from the surface down to bedrock  
232 or groundwater is a unique and important approach for measuring soil or sediment  
233 thickness, hydraulic properties, C storage, and microbiological compositions in the CLP  
234 CZ (Zhu et al., 2018; Jia et al., 2018, 2020; Kong et al., 2022; Wang et al., 2024). At  
235 the pixel grid or sub-watershed scale, methods such as cosmic-ray soil moisture  
236 observing system (COSMOS), neutron probe networks, meteorological stations, and  
237 unmanned aerial vehicle (UAV), amongst others, have been utilized. In addition to  
238 neutron probe networks and UAV remote sensing, meteorological station networks and  
239 hydrological observation stations are also employed at the watershed scale. At the



240 regional scale, apart from the neutron probe and meteorological station network, a  
241 hydrological observation network, field sampling, and satellite remote sensing methods  
242 are also used to investigate soil and water processes over the entire CLP.

243 Specifically, in each watershed CZO, multiple observation approaches have been  
244 applied to support monitoring needs (Fig. 4). Permanent instrumentation includes  
245 automatic meteorological stations, eddy covariance systems (for CO<sub>2</sub>, water vapor, and  
246 heat exchange fluxes), water balance observation fields, and lysimeter clusters  
247 containing typical vegetation types for the measurement of biosphere-atmosphere-  
248 hydrosphere exchange processes. The meteorological systems record key parameters,  
249 including precipitation, air temperature, relative humidity, air pressure, net radiation,  
250 wind speed, and direction. Field observation experiments have been performed in  
251 various land use types in each watershed to monitor critical water processes components  
252 such as soil water content, evapotranspiration (ET), and runoff. Various runoff plots  
253 with different land use types monitor slope runoff and sediment yield. Neutron probes  
254 and COSMOS have been installed in each watershed to evaluate the spatiotemporal  
255 dynamics of soil moisture (Jia et al., 2013, 2015; Wang et al., 2019a; Liu et al., 2023a).  
256 Groundwater level monitoring wells have been installed in each watershed, and soil  
257 hydraulic properties, such as soil saturated hydraulic conductivity and porosity, in  
258 addition to root distributions have been surveyed (Cheng et al., 2009; Gao et al., 2012;  
259 Jian et al., 2014). Precipitation reduction and fertilization experiments are performed to  
260 study the responses of ecohydrological and biogeochemical processes to climate change  
261 (Jia et al., 2012, 2014; Wei et al., 2016b). Forest hydrological processes, including  
262 throughfall, forest interception, stem flow, tree transpiration, and soil water evaporation,  
263 have been observed in the forest ecosystem mainly by rain gauges, interception gauges,  
264 sap flow monitors (thermal dissipation probes, TDPs), and evaporation dishes installed  
265 according to established canopy gap fractions (Wang et al., 2019b). Geophysical  
266 methods, such as electrical resistivity tomography (ERT) (Liu et al., 2023b) and  
267 electromagnetic induction (EMI) (Turkeltaub et al., 2022), have been used to  
268 characterize soil physical properties (soil water content and structure) and infer salt  
269 accumulation in soils. Borehole drilling and soil pit methods are used to evaluate deep

270 soil processes and the variability of loess properties in the vertical dimension (Jia et al.,  
271 2018, 2020; Qiao et al., 2018), allowing for the collection of disturbed and intact soil  
272 samples. Crop/plant (canopy) properties are measured manually or by UAV remote  
273 sensing. A 3-D laser scanner is used to monitor and retrieve gravitational erosion  
274 parameters.

### 275 **3. The CLP as an Ideal Loess CZ**

#### 276 **3.1. Location of the CLP**

277 The CLP is situated in the upper and middle reaches of the YR Basin, bordered by  
278 the eastern Taihang Mountain, western Riyue-Helan Mountain, northern Yinshan  
279 Mountain, and southern Qinling Mountain (33°43'–41°16'N and 100°54'–114°33'E).  
280 The region covers an area of  $64 \times 10^4$  km<sup>2</sup> with an elevation of 200 to 3000 m above  
281 sea level (Fig. 1b). It is significant for the ecological security of the whole of China,  
282 and it has an abundance of natural resources (e.g., coal, oil, and gas) (Zhao et al., 2013).  
283 Notably, the plateau is not entirely covered by loess due to the effects of soil genesis  
284 and landform (Zhu et al., 2018). The north-western region of the plateau is  
285 predominantly covered by aeolian sandy soil, such as the Mu Us Desert, due to its  
286 proximity to the source zone of dust and limited precipitation. The westernmost part of  
287 the plateau mainly consists of desert soil. The deep and continuous loess deposits are  
288 mainly distributed in the middle reaches of the YR, which is considered to be the core  
289 region of the plateau (Liu, 1985).

#### 290 **3.2. Regional Geomorphology**

291 Intense soil erosion over thousands of years has transformed over 70% of the once-  
292 flat plateau into a region dominated by hills and gullies (Zhao et al., 2013). The unique  
293 morphology of the plateau is largely due to paleogeomorphology and erosion intensity.  
294 The typical landforms in this area include Yuan, Liang, Mao, as well as various hills  
295 and gullies of varying degrees of erosion (Fig. 5). Yuan refers to a high, flat, loess  
296 tableland that is not affected by river incisions. In contrast, Liang (a long range of ridges)  
297 and Mao (an oval or round loessial hill) are the result of fluvial and hill-slope erosion,

298 respectively (Yang et al., 2009). As most of the Mao loess evolved from Liang loess  
299 under further erosion, Liang and Mao formations coexist in many areas and are the most  
300 common landscapes on the plateau. In addition, a large number of check dams and  
301 terraces have been constructed on the CLP as effective soil and water conservation  
302 practices (Fig. 5). These hydraulic engineering structures alter the microtopography of  
303 the land surface and offer several attractive advantages, including biodiversity  
304 conservation (Jia et al., 2011), water cleaning (Meninno et al., 2020), enhanced  
305 groundwater recharge (Luo et al., 2020; Zhao and Wang, 2021), flood damage  
306 mitigation (Wei et al., 2016a), C sequestration (Yao et al., 2022), and reduction in  
307 nutrient export loads by runoff to local water bodies (Meninno et al., 2020).  
308 Furthermore, check dam sediments form fertile flat agricultural areas with abundant  
309 nutrients and water to promote vegetation growth and to support livestock (Wen and  
310 Zhen, 2020; Yao et al., 2022).

### 311 3.3. Climate Change

312 A temperate, arid, and semiarid continental monsoon climate dominates the LPC  
313 region. The mean annual temperature in the region ranges from 3.6 to 14.3 °C, while  
314 the mean annual precipitation ranges from 150 to 800 mm. Most precipitation (55–80%)  
315 falls between June and September and decreases along a southeast-to-northwest  
316 transect (Wang et al., 2012). Over the last 60 years, the region-averaged annual mean  
317 temperature has significantly increased from 1960 to 2020 (1.74 °C,  $p < 0.05$ ), with an  
318 increasing rate of  $0.29 \pm 0.1$  °C per 10 years (Fig. S1). This warming trend is over two  
319 times greater than the northern hemisphere average (0.85 °C) and the global average  
320 (0.72 °C) during 1961–2010 (Wang et al., 2012). The annual precipitation was quite  
321 steady between 1960 and 2000, but it increased at a rate of 36 mm per 10 years between  
322 2000 and 2020 ( $p < 0.05$ ) (Fig. S1).

### 323 3.4. Loess Thickness

324 Soil or sediment thickness is a fundamental parameter in CZ science studies, but  
325 its accurate estimation is challenging, especially in areas with deep soil or sediment.

326 Determining soil or sediment thickness can be used to confirm the boundary of soil-  
327 water processes, which is crucial for investigating and modeling hydrological-  
328 biogeochemical processes in the CZ, together with estimations of water, C, and N  
329 reservoirs. Combining borehole drilling from the land surface down to bedrock (56–  
330 205 m) at five sites from south to north of the CLP and analyzing the elevation  
331 difference between the position of bedrock downstream and the adjacent flat loess hills  
332 of 162 sites across the CLP, [Zhu et al. \(2018\)](#) found that the loess thickness over the  
333 plateau mostly ranges from 0 to 350 m, with a mean value of 92.2 m. The mean  
334 thickness of the unsaturated and saturated zone across the CLP is approximately 54.8  
335 and 37.4 m, respectively ([Fig. 6](#)).

### 336 **3.5. Large Variations in Soil Hydraulic Property Values Exist within the VZs**

337 Soil hydraulic properties, including saturated hydraulic conductivity ( $K_s$ ),  
338 saturated soil water content ( $\theta_s$ ), and soil water retention curve  $\theta(h)$ , are critical for  
339 modeling hydrological-biogeochemical processes ([Vereecken et al., 2022](#)). Despite  
340 receiving increasing attention in recent years, data on high-quality soil hydraulic  
341 properties in the deep subsurface remains scarce due to challenges associated with  
342 sampling. Therefore, measured hydraulic properties from the surface layer often  
343 represent those of the deep unsaturated soil to simulate water flow and solute transport  
344 ([Turkeltaub et al., 2018](#); [Hu et al., 2019](#)). If the hydraulic properties exhibit small  
345 variability throughout the soil profile, using uniform representative profiles in a model  
346 may be justified. Additionally, pedotransfer functions (PTFs) can be used to estimate  
347 soil hydraulic parameters in equations related to soil heat flow and biogeochemical  
348 parameters from readily available soil properties, such as particle size distribution  
349 ( $PSD$ ), bulk density ( $BD$ ), and organic C content ([Vereecken et al., 2022](#)). While PTFs  
350 are widely used, most have only been developed for specific regions and may not be  
351 applicable to pedoclimatic conditions for which they are not validated ([Paschalis et al.,](#)  
352 [2022](#)). Since loess deposits are thick and direct measurements of hydraulic properties  
353 are often rare, determining hydraulic property values based on soil hydraulic functions  
354 estimated by PTFs combined with borehole drilling has been a common approach used

355 by loess CZ hydrologists.

356 To develop effective PTFs to estimate soil hydraulic properties of the CLP CZ,  
357 intensive sampling sites over the CLP were selected to collect both undisturbed and  
358 disturbed soil samples from the 0.2–8 m soil layer (Zhao et al., 2020; Niu et al., 2021;  
359 Bai et al., 2022). Soil physical properties [e.g.,  $PSD$ ,  $BD$ , porosity,  $K_s$ ,  $\theta_s$ , and  $\theta(h)$ ] and  
360 organic C content were determined. The van Genuchten (VG) model was used to  
361 describe  $\theta(h)$  relationships, and VG parameters, including  $\alpha$ ,  $n$ , and residual water  
362 content  $\theta_r$ , were determined by fitting the model to the measured retention curve data.  
363 Based on  $PSD$ ,  $BD$ , and other environmental variables, various PTFs were established  
364 to estimate  $K_s$ ,  $BD$ ,  $\theta_s$ ,  $\theta_r$ ,  $\alpha$ , and  $n$  of the loess CZ. Compared with other PTFs, including  
365 the widely used Rosetta PTF (Schaap et al., 2001), the estimation accuracy of the new  
366 PTFs increased by 25–67% (Bai et al., 2022). Notably, compared with others, the new  
367 PTFs have better performances for deep soil layers. To create a regional distribution  
368 map of various soil hydraulic properties, disturbed soil samples from 0–5 m soil layer  
369 at another 243 sampling sites were collected across the CLP (Cao et al., 2018; Zhao et  
370 al., 2019). The new PTFs were then used to estimate soil hydraulic properties at the 243  
371 sampling sites for the 0–5 m soil layer. Spatial distribution maps (1 km  $\times$  1 km) of soil  
372 hydraulic properties within different soil layers across the plateau were generated using  
373 geostatistical spatial interpolation via ordinary-kriging (Fig. 7).

### 374 **3.6. On the Importance of Water Stored in the Loess CZ**

375 Water stored in the VZ, as the primary source of plant available water, is critical  
376 to hydrologic processes on the land surface (Vereecken et al., 2015, 2022). It also  
377 impacts the transport of solutes and other substances in the soil. Understanding the  
378 magnitude and distribution of water storage in the root zone and in the deep VZ is  
379 essential for managing water resources and ecosystems. In this context, a VZ water  
380 observation network was established in 2012 on the CLP (Fig. 8a).

381 Based on *in situ* water observations and simulations, the magnitude and  
382 distribution of VZ water on the CLP have been quantified. For the loess region covering  
383 an area of  $37 \times 10^4$  km<sup>2</sup>, the total water storage capacity in the VZ (with a region-

384 averaged VZ thickness of 54.8 m) was estimated to be approximately  $3.1 \times 10^{12} \text{ m}^3$ ,  
385 equivalent to a 9.6-m thick layer of water covering the land surface of the region (Zhu  
386 et al., 2019). The total water storage capacity is equal to an accumulation of 20 years of  
387 mean annual precipitation (1963–2012) across the CLP. The central parts of the region  
388 have the highest VZ water storage. In contrast, the northwest and southeast parts have  
389 relatively low VZ water storage (Fig. 8b), mainly depending on VZ thickness and  
390 precipitation. In addition, the total water storage in the 0–5 m soil layer (the root zone)  
391 of the plateau was approximately  $2.7 \times 10^{11} \text{ m}^3$ , of which 42% is available for plants  
392 (total water storage minus water storage at the wilting point) (Cao et al., 2018; Zhao et  
393 al., 2021). Plant-available soil water storage in the 0–5 m soil layer (ranging between 0  
394 and 1110 mm, with a mean of 306 mm) generally decreases from the southeast to the  
395 northwest of the region (Fig. 8c), and it is mainly influenced by soil texture and  
396 precipitation (Zhao et al., 2021). Moreover, we deduced the water resource composition  
397 across the CLP from the estimates of the VZ and saturated zones water and the runoff  
398 discharge data. The water resources composition of the CLP comprises precipitation,  
399 river water, VZ water, and saturated zone water (shallow groundwater), accounting for  
400 2.1, 0.1, 42.1, and 55.7%, respectively, suggesting an overwhelming fraction (97.8%)  
401 of water resources in the thick loess profiles of the CLP CZ (Zhu et al., 2019).

### 402 **3.7. Importance and Uniqueness of CLP in CZ Research**

403 The CLP holds the distinction of being both the largest and deepest loess deposit  
404 in the world, which today supports a population of 117 million people, accounting for  
405 about 36.4% of the total population residing in the loess regions of the world. It covers  
406 about 6.7% of China's land area and supports over 8.5% of China's population. The  
407 CLP has experienced long-term intensive agricultural disturbances (spanning more than  
408 2000 years), extensive vegetation restoration, and engineering practices, such as check-  
409 dam construction and terracing. These activities have significantly altered the land-  
410 cover and geomorphic features of the plateau and, consequently, the CZ processes,  
411 functions, and services. Additionally, the CLP is one of the most impoverished regions  
412 in rural China and requires urgent action to improve environmental sustainability and

413 promote economic growth and welfare in the face of natural resource limitations  
414 (Sjögersten et al., 2013). Thus, the CLP is one of the ideal regions in the world to study  
415 CZ science under highly managed or disturbed conditions. The CLP CZO consists of a  
416 longitudinal series of monitoring sites rather than a single observatory sub-catchment  
417 (Fig. 1b). This larger scale, multi-catchment approach facilitates a regional  
418 comprehensive understanding of CZ processes and services that encompass spatial  
419 variations in landscape properties, land management, and social-economic conditions  
420 (Naylor et al., 2023).

#### 421 **4. Answers to the Scientific Questions based on Results from Loess CZs**

##### 422 **4.1. Can Soil Erosion be Controlled or Alleviated?**

423 Soil conservation is one of the most important loess *CZ supporting services*,  
424 directly affecting food production and eco-environmental security of the CZs. Over the  
425 past 2,000 years of agricultural reclamation, most forests were cleared for farmland to  
426 feed the growing human population on most of the loess CZs, particularly on the CLP.  
427 Historical records show that forest coverage on the CLP steadily declined as the  
428 population increased, with forest cover dropping from approximately 40% during the  
429 time of the North-South dynasties (420–589 CE) to 33% during the Tang and Song  
430 dynasties (618–1279 CE). By the time of the Ming and Qing dynasties (1368–1911 CE)  
431 and the formation of the People’s Republic of China (in 1949), only between 15% and  
432 6% of the forests remained (Xu, 2001). Changes in land use resulted in annual sediment  
433 delivery to the YR increasing from about 0.2 billion tons in the 11<sup>th</sup> century CE to 0.6  
434 billion tons in the 14<sup>th</sup> century CE. Population growth and reclamation activities  
435 continued to increase until 1950 CE, when annual sediment discharge peaked at about  
436 1.6 billion tons, which made the YR the world’s largest contributor of fluvial sediment  
437 load. Muddy floods due to agricultural runoff were also a widespread and frequent  
438 phenomenon in the European loess belt (Boardman et al., 1994), especially in Northern  
439 France (Souchère et al., 2003), UK (Boardman et al., 2003) and central Belgium (Evrard  
440 et al., 2008). These floods were triggered when high runoff was generated on  
441 agricultural land causing severe erosion.

442 Various government conservation and restoration strategies have been  
443 implemented during the past decades to control soil erosion and rehabilitate the  
444 degraded ecosystems on the CLP, including the “Grain-for-Green Program” (GfGP,  
445 1999–2020). As a result, vegetation coverage on the CLP has increased from 32% in  
446 1999 to 63% in 2018 (Hu and Zhang, 2020). The combination of increased vegetation  
447 coverage and engineering measures such as check-dams, terraces, level furrows, and  
448 fish-scale pits has effectively reduced soil erosion on the CLP, with the annual sediment  
449 discharge into the YR decreasing from 1.6 billion tons in the 1950s to about 0.2 billion  
450 tons in 2015 – similar to historic levels (Chen et al., 2015; Wang et al., 2016a). About  
451 80% of the decline in annual runoff for the YR has been attributed to human activities,  
452 including the GfGP, river dam projects, terracing, agricultural irrigation, and other  
453 water conservation projects (Liu et al., 2020a). In addition to re-establishing a closed  
454 vegetation cover, a high plant functional diversity also played an important role in  
455 reducing soil erosion in degraded ecosystems. Runoff experimentations performed in  
456 the European loess belt (Kervroëdan et al., 2019) and the CLP (Zhu et al., 2015b)  
457 showed that multi-specific communities could be used to mitigate soil erosion, and  
458 plant species and functional diversity also offered other ecosystem processes and  
459 services.

460 To protect agricultural soils from erosion, practices such as intercropping and  
461 straw mulching are widely used in cultivated loess regions. For instance, intercropping  
462 a pecan agroforestry practice with a perennial legume such as kura clover on deep loess  
463 soils of the Missouri River hills landscape offers an effective alternative management  
464 system to optimize alley crop production while promoting soil conservation (Kremer  
465 and Kussman, 2011). Ridge-tillage is more effective than conventional (moldboard  
466 plowing or disking) tillage in reducing sediment loss from watersheds through the  
467 physical retention of runoff and increasing the baseflow in the loess hills of southwest  
468 Iowa (Kramer et al., 1999; Moorman et al., 2004), while Triplett et al. (1996) suggested  
469 that no-tillage production systems can be developed for highly erosive loess soils in the  
470 U.S. Mid-South. Furthermore, various natural and organic mulches (e.g., crop residues,  
471 leaf litter, woodchips, bark chips, biological geotextiles, gravel, crushed stones, biochar,



472 and polyacrylamide) have also been used to protect the loess land surface against the  
473 erosive forces of rain and runoff (Guo et al., 2010; Sadeghi et al., 2021). Using stone  
474 and gravel mulches in the semi-arid loess region of northwestern China has been an  
475 indigenous farming technique for crop production for over 300 years (Li, 2000).

476 In summary, soil erosion in cultivated loess areas around the world has been  
477 mitigated through the implementation of various restoration programs and conservation  
478 management practices. Despite this success, soil erosion remains one of the most  
479 pressing environmental issues in loess regions, and the regional ecosystem remains  
480 fragile. Soil erosion under extreme precipitation events must receive additional  
481 attention in the future (Ciampalini et al., 2020; Doulabian et al., 2021).

#### 482 **4.2. Does a Large-Scale Ecological Program Affect Local Food Security?**

483 Food supply is closely related to a region's economy and people's livelihoods  
484 (Enenkel et al., 2015; Folberth et al., 2020), and is a major CZ *provisioning service*.  
485 The cultivated land area is one of the most important factors for total grain production.  
486 Due to the growing human population living on loess soil or other CZs, forests are often  
487 converted into farmland to ensure food supply. Interestingly, with the large-scale  
488 conversion of farmland to natural land (i.e., grassland and woodland) to protect the  
489 degraded ecosystem in some loess CZs, particularly in the CLP, new problems such as  
490 food insecurity and water shortage have emerged due to the occupation of farmland and  
491 the depletion of soil water by the large-scale revegetation programs (Chen et al., 2015).  
492 Such problems may hinder a region's sustainable development of the eco-environment  
493 and social-economy. To date, the revegetation programs have converted more than  
494 30,000 km<sup>2</sup> of rain-fed cropland to forest or grassland on the CLP (Feng et al., 2016;  
495 Shi et al., 2020). Consequently, the total grain output of the CLP decreased from 23.8  
496 million tons in 1998 to 16.7 million tons in 2001. The corresponding grain self-  
497 sufficiency index (GSSI, an index to assess a region's ability to generate enough grain  
498 to support its population) of the CLP also dropped sharply from 0.88 in 1998 to 0.60 in  
499 2001 (Zeng et al., 2022). When the GSSI value is less than 0.90, the risks for regional  
500 grain shortages increase (Mukhopadhyay et al., 2018). Shi et al. (2020) report mounting

501 pressures on CLP croplands from 1999–2010, with the annual grain yield loss by the  
502 GfGP increasing from 0.40 million tons in 1999 to 3.47 million tons in 2010. Although  
503 the GSSI has shown a significant upward trend in the region with the continuous  
504 adjustment of policies in recent years, the 2015 GSSI value (0.83) in the region was less  
505 than 0.90 (Zeng et al., 2022). The reduction in grain production caused by excessive  
506 vegetation restoration will inevitably threaten the survival and development of farmers,  
507 particularly in the loess mountainous areas (Chen et al., 2015; NFGA, 2020). Therefore,  
508 it is possible that too much grain has been traded for green, and land use on the CLP  
509 must be re-balanced to avoid exacerbating food shortages in local communities (Chen  
510 et al., 2015; Wang et al., 2021a).

511 Increasing grain production per unit area through promoting intensive agriculture,  
512 creating new farmland (e.g., terraces, check dam fields), improving the quality of  
513 cultivated land, and increasing water and fertilizer use efficiencies can help increase  
514 grain production (Liu et al., 2013; Zheng et al., 2020). The construction of terraces and  
515 check dams significantly contribute to grain production on the CLP. From 1999 to 2007,  
516 the terraced and check dam field area increased from 1,477 and 181 km<sup>2</sup> to 7,644 and  
517 690 km<sup>2</sup>, respectively (Gao et al., 2016). The contribution of terraces and check dam  
518 fields to grain yield increased from 0.34 million tons in 1999 to 1.69 million tons in  
519 2007 (Shi et al., 2020). By 2018, the terraced field area increased to 3.7×10<sup>4</sup> km<sup>2</sup>. More  
520 than 55,000 check dams were constructed on the CLP between 1960 and 2010, and  
521 these dams captured approximately 21 billion m<sup>3</sup> of sediments (Jin et al., 2012; Fu et  
522 al., 2017). The Chinese government plans to build 15,000 more check dams on the CLP  
523 between 2020 and 2035. Terraces and check dams not only help to conserve soil and  
524 water but also lead to increased grain production, resulting in an increase in grain self-  
525 sufficiency.

526 In summary, extensive vegetation restoration on CLP farmlands can threaten local  
527 food security. Appropriate vegetation restoration strategies and multiple policies (e.g.,  
528 construction of terraces and check dams and improvements to the agricultural  
529 production conditions) should be implemented to increase grain production in order to  
530 achieve a win-win situation for Grain and Green areas.

### 531 4.3. Does Large-Scale Vegetation Restoration Exacerbate Water Scarcity?

532 Agricultural production and ecological construction on the loess CZs rely heavily  
533 on water resources. As a result, water supply is a major *CZ provisioning service* that is  
534 constantly impacted by changes in land use and land cover. In the CLP, the significant  
535 increase in vegetation coverage has increased ET but reduced runoff and soil moisture  
536 (Feng et al., 2016; Jia et al., 2017a, b; Luan et al., 2022). Such contrasting effects  
537 aggravate water resource shortages in arid and semi-arid loessial regions. In the CLP,  
538 the regional ET increased at a rate of  $4.3 \pm 1.7 \text{ mm yr}^{-1}$  from 2000 to 2010, while soil  
539 moisture and runoff decreased at a rate of  $2.4 \pm 0.9 \text{ mm yr}^{-1}$  and  $0.5 \pm 0.3 \text{ mm yr}^{-1}$ ,  
540 respectively (Feng et al., 2016). Although recent observations report that runoff  
541 increased at a rate of  $2.4 \text{ mm yr}^{-1}$  from 2011 to 2020 due to a significant increase in  
542 precipitation, ET also exhibited an upward trend in most areas of the CLP, with an  
543 increasing rate of  $5.7 \text{ mm yr}^{-1}$  (Cao et al., 2023; Lu et al., 2024). Overall, the recharge  
544 amount was generally less than the discharge amount in the CLP from 2001 to 2020,  
545 mainly due to large-scale revegetation, and the difference between recharge and  
546 discharge was gradually expanding, with a change rate of  $-0.58 \text{ mm yr}^{-1}$  (Lu et al.,  
547 2024).

548 Soil water is the primary limiting factor and driving force behind vegetation  
549 growth and ecosystem functioning in the loess CZ (Jia et al., 2017a, b). Unreasonable  
550 revegetation practices, which include the extensive introduction of exotic deep-rooted  
551 high-water-demanding plant species or over-planting, can result in excessive  
552 consumption of deep soil water (Wang et al., 2010, 2011, 2015a; Jia et al., 2017a; Ge  
553 et al., 2020). A recent integrative study has shown that land use conversion from arable  
554 cropland to forest/grassland caused an 18% decrease in soil water in the 0–18 m profile  
555 across the CLP over the past 37 years (1985–2021), with a greater declining rate in the  
556 semi-arid region (21%) than in the semi-humid region (15%) (Wang et al., 2024),  
557 inducing deep soil desiccation and dry soil layers (DSLs) formation. The formation of  
558 a DSL can interfere with the water cycle in the groundwater-soil-plant-atmosphere  
559 continuum by preventing water flow between shallow and deep soil layers and may

560 decrease groundwater recharge (Li et al., 2018a, 2019a; Huang et al., 2021). For  
561 instance, in the southern CLP region, the conversion of cropland (shallow-rooted) to  
562 apple orchards (deep-rooted) decreased soil water storage in the 0–18 m profile by 776,  
563 1106, and 1117 mm, corresponding to 19, 20, and 26-year-old apple orchard,  
564 respectively (Li et al., 2018a). Similar results were reported by Wang et al. (2015a) that  
565 soil moisture in the 0–18 m profile decreased with increasing ages of apple orchards at  
566 Wangdonggou watershed CZO. There was a significant decline in potential  
567 groundwater recharge following the land-use change (Zhang et al., 2018b).

568 Prolonged soil desiccation can reduce drought resistance of plants and limit  
569 vegetation growth and natural succession, and may even result in tree mortality (Wang  
570 et al., 2010, 2011; Gao et al., 2021a; Shao et al., 2023; He et al., 2023). For instance,  
571 during the 2012–2015 drought in California, particularly in the southern Sierra Nevada  
572 area, forest die-off was found to be closely tied to multi-year deep-rooting-zone (5–15-  
573 m depth) drying (Goulden and Bales, 2019). It has been widely observed that the  
574 aboveground growth of planted trees is greatly constrained by deep soil desiccation on  
575 the CLP, resulting in so-called “small old trees”, where some 30-year-old forest trees  
576 only grow to about 20% of their normal height (Fang et al., 2016; Jia et al., 2017a).  
577 Recent studies in the CLP have shown that when the soil below a depth of 2 m is dry,  
578 the canopy transpiration and the net photosynthetic rate of apple trees are reduced,  
579 respectively, by around 40% and 20% relative to that without deep soil desiccation (Li  
580 et al., 2021; Yang et al., 2022). Additionally, embolism resistance increases with a  
581 decrease in soil water availability, leading to a reduction in xylem hydraulic  
582 conductivity and even hydraulic failure of the plantation (Liu et al., 2020b; Fuchs et al.,  
583 2021). Furthermore, soil desiccation significantly and negatively affects microbial  
584 community structure and functionality in deep soils, with substantially decreased  
585 bacterial beta diversity and decreased network robustness in deep soils (120–500 cm)  
586 where a DSL occurs (Kong et al., 2022).

587 Achieving optimal plant coverage, which refers to the maximum leaf area index  
588 that can be achieved without causing soil water to dry to the wilting, requires a critical  
589 balance of water consumption and eco-environmental service performances for a

590 revegetation program (Fu et al., 2012). Scientists and resource managers who are  
591 concerned about the optimization of plant coverage often invoke the concept of *soil*  
592 *water carrying capacity for vegetation* (SWCCV), which has been defined as “the  
593 maximum biomass of a given vegetation type, under specific climatic conditions, soil  
594 texture, and management regime that a given arid or semiarid area can sustain without  
595 diminishing soil water capacity to support future generations” (Xia and Shao, 2009).  
596 Several studies have been done on SWCCV of different plant species using field-  
597 observations and model simulations at various scales (Xia and Shao, 2008; Zhang et al.,  
598 2015, 2018a, 2024; Jia et al., 2019). At the watershed scale, Xia and Shao (2008)  
599 developed a physically-based model that builds on the concept of an equilibrium  
600 adjustment of plant growth to soil water dynamics. At the regional scale, Jia et al. (2019)  
601 determined the optimal plant coverage for non-native plants mainly used in the CLP  
602 revegetation program using a modified Biome-BGC model. Eagleson’s ecohydrological  
603 optimality method (Eagleson, 2002) and the Shuttleworth-Wallace model (Ortega-  
604 Farias et al., 2010) were also used to determine the maximum plant coverage over the  
605 CLP (Zhang et al., 2018a; Li et al., 2023b). They found that the current vegetation cover  
606 has already exceeded the climate-defined equilibrium vegetation cover in many parts  
607 of the plateau. This suggests that there was extensive over-planting in those areas where  
608 the local limited precipitation did not effectively support revegetated plants, and  
609 additional vegetation plantation will cause a water supply shortfall for human activities  
610 (i.e., an unsustainable situation).

611 Although there are ongoing efforts to understand the vegetation productivity  
612 threshold, equilibrium vegetation coverage, and SWCCV, the consistency of  
613 revegetation thresholds obtained by different methods remains uncertain. A serious  
614 challenge exists to address the contradiction between water shortages and eco-  
615 sustainability due to climate change and human activities. Future research should focus  
616 on comparative studies of different methods to determine the upper limit of vegetation  
617 restoration under the influence of climate change and human activities (e.g., agricultural  
618 and industrial water use).

619 In summary, excessive large-scale anthropogenic revegetation enhances water

620 consumption and exacerbates water scarcity in loess CZs. The continued decline in  
621 available water resources will further exacerbate the limitation of water on the CZ  
622 service, jeopardizing its current stability and future ecological and socioeconomic  
623 sustainability. It is essential to determine critical revegetation thresholds to control soil  
624 erosion without negatively impacting water availability, thereby ensuring a sustainable  
625 ecohydrological environment in the loess CZs.

#### 626 **4.4. Can Desiccated Deep Soils be Hydrologically Recharged and Restored?**

627         Given the significant negative effects of deep soil desiccation on ecological and  
628 hydrological processes (see section 4.3), immediate action to remediate DSLs is  
629 required. Field experiments and numerical model simulations have been performed to  
630 evaluate water recovery in desiccated deep soils. It has been acknowledged that  
631 negative ecohydrological impacts of soil desiccation can be partly alleviated through  
632 rational management measures, such as thinning, pruning, or changing vegetation type  
633 and structure. These measures not only significantly decrease water loss by reducing  
634 ET but also improve deep soil water recharge, thus ensuring water supply for plants  
635 under drought conditions (Ma et al., 2019; Wang et al., 2020, 2023a). For example, a 2-  
636 year field experiment situated in a semi-arid loess hilly area of the CLP showed that  
637 thinning the stand density by 67% or pruning 25% of the branches significantly  
638 promoted plant rejuvenation and improved soil water use efficiency for a degraded *C.*  
639 *korshinskii* plantation resulting from overplanting (Wang et al., 2023a).

640         The replacement of exotic trees and shrubs by native grasses or crops also benefits  
641 water recovery in desiccated deep soils. Huang and Gallichand (2006) showed that soil  
642 water levels in the 0–10 m soil layer were recovered in 6.5–19.5 years after replacing a  
643 30-year-old apple orchard with winter wheat in the southern CLP. A 5-year field  
644 experiment in the northern CLP showed that water content in the 0–8 m soil profile  
645 increased drastically after alfalfa was replaced by soybean, especially after consecutive  
646 wet years when the soil water content of the 0–8 m profile was recharged up to 0.16  
647 cm<sup>3</sup> cm<sup>-3</sup> (Ge et al., 2022). Simulation results for the semi-arid grass zone of the CLP  
648 showed that a 5 m thick DSL could recover 2–13 years after replacing artificial

649 forests/shrubs with natural grasses, while the time of soil water recovery depended on  
650 the degree of soil desiccation, soil hydraulic properties, and slope within a specific  
651 climatic zone (Bai et al., 2021).

652 Moreover, slope engineering measures such as infiltration holes (Wang et al., 2020;  
653 Zhang et al., 2023), fish scale pits (Wang et al., 2021b), and rainwater collection and  
654 infiltration systems (Song et al., 2020) can contribute to intercepting runoff and  
655 increasing deep soil water replenishment, which helps to mitigate soil desiccation  
656 induced by overplanting. For example, Yang et al. (2023) found that integrating various  
657 slope engineering measures significantly increased soil water storage, organic C, and  
658 total nitrogen (N), and promoted plant growth in a degraded *Prunus davidiana*  
659 plantation. Heavy rainfall events (>50 mm) are also conducive to water infiltration into  
660 desiccated deep soils, indicating the possibility of DSL recovery under natural  
661 conditions (Shi et al., 2021; He et al., 2022).

662 In summary, desiccated deep soils caused by excessive plant water uptake can be  
663 recharged and restored through rational management measures, including vegetation  
664 management and slope engineering measures. In this way, the vegetation does not only  
665 decrease surface runoff, but also increases infiltration rate, ultimately conserving soil  
666 and water and improving the microclimatic environment.

#### 667 **4.5. Does Precipitation Recharge Groundwater in Thick Loess CZs?**

668 Groundwater is the primary drinking water source in many loess CZs.  
669 Groundwater recharge (GR) indicates the existence of renewable groundwater  
670 resources and is an important component of the sustainability of CZ services (Moeck et  
671 al., 2023). However, GR largely varies in space and time and is difficult to measure  
672 directly. Furthermore, the spatial parameterization of hydrological modeling to estimate  
673 GR in loess CZs is challenging and is subject to high uncertainty (Turkeltaub et al.,  
674 2018).

675 Loessial soils are regarded by many as transmissive and rechargeable (Lin and Wei,  
676 2006; Seiler and Gat, 2007). Assessment of recharge rates under loessial soils for  
677 various climates and vegetation has been investigated through infiltration experiments

678 and numerical modeling (Baran et al., 2007; Gvirtzman et al., 2008; Dafny and Šimůnek,  
679 2016; Turkeltaub et al., 2018). On the CLP, modeling results indicate significant spatial  
680 variations in GR fluxes, with relatively high GR in the south area of the plateau,  
681 characterized by concentrated irrigated agricultural fields, more moderate GR in the  
682 north parts of the plateau, and low GR in the center of the region (Turkeltaub et al.,  
683 2018; Hu et al., 2019). Additionally, the transition from cropped fields to forest and  
684 grassland has caused a reduction of 6.1% in the total annual recharge between 1975 and  
685 2008. However, changes in GR do not always occur simultaneously with land-use  
686 conversions, and delays may be influenced by the VZ thickness, soil texture, climate,  
687 and water input frequency and quantity. In areas with thin VZs, recharge generally  
688 decreases with a cropland-to-forestland conversion, consistent with findings reported  
689 by Dafny and Šimůnek (2016) that recharge rates decrease with an increase in the  
690 vegetation cover under sandy loess deposits (~20 m) south of the Gaza Strip.  
691 Additionally, the time lag between specific rainy seasons and corresponding recharge  
692 events increases with increasing vegetation cover. However, at many CLP sites, the VZ  
693 is relatively thick, and precipitation takes a relatively long time to recharge groundwater.  
694 Nevertheless, to examine the potential effects of climate change and land-use change  
695 on GR, a long-term climate and land use database is required, or alternatively, stochastic  
696 methods can be used to construct long climate records (Turkeltaub and Bel, 2023).

697       Precipitation can recharge shallow groundwater by a dual process consisting of  
698 infiltration via various preferential flow pathways (e.g., macropore, crack, burrow,  
699 finger, and lateral flows) in response to heavy precipitation, followed by a piston-like  
700 (or uniform) flow (Manna et al., 2017). The behavior of preferential flow and piston  
701 flow co-evolving within a CZ has been labeled as one of the 23 unsolved problems in  
702 hydrology (Blöschl et al., 2019). Over the past decades, numerous methods, including  
703 infiltration experiments, chloride mass balance, water isotopes (e.g.,  $^3\text{H}$ ,  $^2\text{H}$  and  $^{18}\text{O}$ ),  
704 and numerical modeling have been used to quantify dual recharge mechanisms in the  
705 deep VZ of the loess CZs (Baran et al., 2007; Gvirtzman et al., 2008; Huang and Pang,  
706 2011; Huang et al., 2017, 2020; Hu et al., 2019; Li et al., 2017, 2019a; Lu et al., 2020;  
707 Xiang et al., 2019, 2020; Shi et al., 2021; Gao et al., 2023). Despite extensive research,



708 precise identification of the recharge mechanisms remains elusive. Some studies have  
709 identified piston flow as the dominant GR mechanism after investigating signatures of  
710 multiple tracers from a thick VZ and underlying saturated zone (Baran et al., 2007;  
711 Huang and Pang, 2011; Huang et al., 2017, 2020; Xiang et al., 2019; Shi et al., 2021).  
712 In numerical simulations, piston flow is generally assumed to be the dominant water  
713 transfer mechanism in layered loess deposits (Dafny and Šimůnek, 2016; Turkeltaub et  
714 al., 2018). Conversely, preferential flow was identified as a dominant mechanism in the  
715 Luochuan and Changwu highland areas (with a VZ thickness of 40–80 m) (Wang, 1982;  
716 Yan, 1986; Xu and Chen, 2010) and Heihe watershed (with a VZ thickness of 30–100  
717 m) (Li et al., 2017) on the CLP. Similar results were also observed in the western CLP  
718 (Tan et al., 2016), likely due to sinkholes and slip surfaces or landslide surfaces.  
719 However, results from Huang et al. (2019) indicated a combination of GR mechanisms  
720 in deep loess deposits. Tracers in the VZ suggested piston flow, while detectable tritium  
721 in the VZ implied preferential flow. Some other GR mechanisms in loess CZs have also  
722 been reported. Gao et al. (2023) employed a coupled liquid–vapor–heat–airflow  
723 STEMMUS (simultaneous transfer of energy, mass, and momentum in unsaturated soil)  
724 model to investigate the impact of extreme precipitation on loess CZ hydrological  
725 processes. They found that thermal-gradient-driven vapor transfer is an important  
726 mechanism for deep-layer recharge in the loess CZ. Hou et al. (2018) considered the  
727 ground-atmosphere interactions and found that water percolation in a thick loess VZ  
728 was in liquid and vapor phases. Furthermore, heterogeneous and layered loess deposits  
729 (e.g., loess-paleosol sequences, alternating silty-sand and sandy-clay loess layers) may  
730 influence deep recharge (Gvirtzman et al., 2008). The above methods are commonly  
731 used to study the GR process in the loess CZs. Considering the complexity and  
732 uncertainty of GR mechanisms, it is necessary to apply multiple methods  
733 simultaneously, rather than a single method, to obtain reliable conclusions.

734 In summary, compared to results from similar loess CZ sites, the primary GR  
735 mechanism differed among sites and may depend on spatial scales, geomorphology, and  
736 landscape (Xiang et al., 2019; Chen et al., 2023). Not enough information has been  
737 collected to fully understand *how* and *when* groundwater is recharged at the regional

738 scale, resulting in this topic emerging as a key research priority. The mechanisms of GR  
739 are highly complex in loess CZs due to the dry climate, thick VZ, complex geomorphic  
740 landscapes, and large vegetation change from shallow- to deep-rooted plants, requiring  
741 further long-term monitoring and investigation. In addition, the mechanisms controlling  
742 water transport (exchange processes, fluxes, and travel times) from root zone to  
743 groundwater and interactions within the groundwater-soil-plant-atmosphere continuum  
744 remain unclear (Fig. 9).

#### 745 **4.6. What Are the Ecohydrological Functions of Weathered Bedrock?**

746 Weathered bedrock is crucial in the Earth's CZ. It connects soil moisture dynamics  
747 and shallow groundwater recharge, and therefore plays an essential role in the  
748 ecohydrological and biogeochemical cycling on the Earth's land surface (Salve et al.,  
749 2012; Rempe and Dietrich., 2018). Rock moisture is a critical component of terrestrial  
750 water and C cycling (McCormick et al., 2021). Weathered bedrock redefines the  
751 hydrological distribution in shallow soils (Hasenmueller et al., 2017; Rempe and  
752 Dietrich., 2018), which directly affects surface infiltration and ET processes (Rathay et  
753 al., 2018; Hahm et al., 2022; Jiménez-Rodríguez et al., 2022). Moreover, bedrock is the  
754 source of most mineral nutrients (e.g., Fe, Ca, P, and other elements), shaping vegetation  
755 growth and community composition (Morford et al., 2011; Jiang et al., 2020).

756 Early studies and field investigations indicate that the vegetation type and  
757 distribution may be related to the upper loess thickness and the underlying bedrock  
758 geological structure on the CLP (Zhang and An, 1994; Zhang et al., 1998). They report  
759 that shallow soil hillsides with coarse-textured weathered bedrock underneath are  
760 suitable for woody vegetation growth. This might be associated with the relatively  
761 humid environment deriving from deep rainwater infiltration and low evaporation  
762 consumption. Similar results are reported for the Elder Creek Watershed CZO in  
763 northern California that up to 27% of the annual rainfall is seasonally stored as rock  
764 moisture, which exceeds soil moisture and is a critical and stable source of plant-  
765 available water in drought years (Rempe and Dietrich, 2018). The thick VZ and  
766 weathered, fractured bedrock (30 m thick at ridgetops) in the CZ at Elder Creek thus

767 allow ample water storage and support for a dense evergreen forest canopy. However,  
768 because of the inaccessibility of the weathered bedrock underlying thick loess deposits  
769 and few direct observations of rock moisture, its hydrologic properties and dynamics  
770 are poorly understood.

771 The emergence of research on the CZ, which extends from the vegetation canopy  
772 through the soil and weathered bedrock has further identified knowledge gaps. Recently,  
773 *in-situ* observations and simulation experiments were performed to investigate rock  
774 core sample characteristics and ecohydrological functions of weathered bedrock at the  
775 Liudaogou Watershed CZO in northern CLP (Luo et al., 2023, 2024). Borehole  
776 investigations showed that weathered bedrock layers had a thickness of more than 5.0  
777 m, and the weathering intensity gradually decreased with depth. The underlying  
778 weathered bedrock is mostly limestone with soft lithology, which provided pathway for  
779 roots to penetrate and extend into bedrock cracks to absorb water and nutrients (Zhang  
780 et al., 1998). Simulation experiments showed that stable infiltration rates increase  
781 linearly with weathered bedrock thickness, which accelerates by 0.5–5.7 times more  
782 than bulk soil layers, whereas cumulative evaporation presents a significant decrease of  
783 7.4–32.8%. Overall, water conditions in profiles with weathered bedrock are better than  
784 those in thicker soil layers, with an average rock moisture twice that of soil moisture.  
785 Moreover, field investigations using UAV orthophotos clearly showed that the  
786 vegetation growth in Wuqi County was better than that in Dingbian County of the  
787 northern CLP (Luo et al., 2023). The main differences were that upper soil layers were  
788 thinner, and underlying weathered bedrock layers were thicker in Wuqi than in  
789 Dingbian. In addition, a field survey found that there was water seepage through the  
790 exposed weathered bedrock layers (Fig. 9), suggesting that the composition of  
791 streamflow (runoff) was influenced by the transit of infiltrating rainfall through meters  
792 of weathered bedrock (Banks et al., 2009; Kim et al., 2017).

793 In summary, weathered bedrock substantially suppresses surface infiltration and  
794 evaporation and plays an important role in mediating vegetation growth and  
795 composition (especially for deep-rooted trees and shrubs) in water-limited loess CZs.

796 Although the loess CZ is a representative landform with a thick layer of loess deposits,  
797 the ecohydrological functions of weathered bedrock should be a focus of CZ science,  
798 particularly integrating moisture storage in weathered bedrock with vegetation,  
799 hydrological, and climate models (Jiang et al., 2020; Lapidés et al., 2024).

#### 800 **4.7. Do Agricultural Practices Impact Groundwater Quality?**

801 Nitrate groundwater contamination is an important issue in many parts of the world  
802 (World Health Organization, 2007). Recent studies at both national and catchment  
803 scales have shown that there can be substantial (and increasing) storage of nitrate in  
804 soils, the VZ, and groundwater (Worrall et al., 2015; Ascott et al., 2016; Meter et al.,  
805 2016). Globally, VZ nitrate storage per unit area is greatest in North America, China,  
806 and Europe, which have thick VZs and extensive historical agriculture activities (Ascott  
807 et al., 2017). The loess CZ is known for its deep soil and long-term extensive agriculture,  
808 which makes it possible to accumulate large amounts of nitrate or other pollutants,  
809 gradually traveling downward and reaching the aquifer. In some cultivated regions of  
810 the CLP, such as the Guanzhong Plain, Changwu and Luochuan tablelands, centuries  
811 of agricultural activities have resulted in significant nitrate accumulation in deep soils,  
812 including contamination of groundwater in some areas (Jia et al., 2018; Huang et al.,  
813 2021; Gao et al., 2021a, b, c; Zhu et al., 2021; Lu et al., 2022; Niu et al., 2022; Ren et  
814 al., 2023). Analyses from five boreholes, for example, showed that the measured nitrate  
815 content in the entire profile at Fuxian, An'sai, and Shenmu is low (Jia et al., 2018). Still,  
816 significant accumulations were observed in the 30–50 m layer at Yangling and  
817 Changwu (Jia et al., 2018). High nitrate accumulations are attributed to large N-  
818 fertilizer applications, long agricultural history, high precipitation coupled with  
819 irrigation, and high atmospheric N deposition rates. Significant nitrate accumulation in  
820 deep soils (~7 m) was also found in an intensively farmed loess area in Obernai, Alsace  
821 (Rhine Valley, France) (Baran et al., 2007).

822 The Guanzhong Plain (GP) is situated in the southern part of the CLP and is  
823 recognized as the birthplace of an ancient Chinese agricultural civilization, where  
824 farmers used organic waste to maintain crop production and soil fertility for thousands

825 of years (Niu et al., 2022). Long-term manure applications led to an anthropogenic  
826 surface layer over the zonal soil profile termed the Lou soil (or Manurial Loessial soil),  
827 the depth of which is 30–100 cm (Zhu, 1964). This may have resulted in nitrate  
828 accumulation, causing environmental pollution of groundwater. For over a millennium,  
829 numerous ancient county annals recorded nitrate-rich groundwater, also known as  
830 nutritive groundwater, in the GP (Gun et al., 2007). The spatial distribution of nitrate-  
831 rich groundwater over the region was first reported in the 1970s prior to chemical  
832 fertilizer applications (Peng et al., 1979).

833 Water quality *regulating services* were impacted by land-use change, such as the  
834 cropland-to-orchard transition in the middle and south parts of the CLP (Gao et al.,  
835 2021a; Lu et al., 2022). Since the 1990s, land-use-pattern changes from cereal croplands  
836 to apple or kiwifruit orchards have been promoted in the GP and other tablelands (e.g.,  
837 Changwu and Luochuan) due to economic benefits. Provincial Yearbook data show that  
838 the total area of orchards in Shaanxi Province increased from 0.10 million ha in 1980  
839 to 1.15 million ha in 2020, with approximately 45% of the area in the GP. This increase  
840 in orchards has significantly reduced rural poverty and improved farmer income (Gao  
841 et al., 2021c). However, compared to croplands, orchards require higher amounts of  
842 irrigation water and N-fertilizers, leading to nitrate entering the deep soils due to an  
843 accelerated leaching rate (Niu et al., 2022) (Fig. 10). This excess nitrate can migrate  
844 vertically towards the groundwater table or horizontally through shallow subsurface  
845 flow, resulting in nitrate accumulation and contamination of downstream water bodies.  
846 For instance, Chen et al. (2019) noted that land-use change from arable lands to  
847 orchards reduced soil erosion but increased nutrient loss in the southern part of the CLP.  
848 Gao et al. (2021b) also found that long-term kiwifruit production deteriorated  
849 groundwater quality in the Yujiahe catchment within the GP. Furthermore, excessive  
850 fertilization has been observed to disturb the acid-base equilibrium in apple orchards,  
851 resulting in significantly lower soil pH than in tree plantations and cropland (Gao et al.,  
852 2021c). This major environmental issue seriously threatens regional environmental  
853 security and the sustainable utilization of water and soil resources in cultivated loess  
854 CZ.

855 Previous studies on N biogeochemical cycling in terrestrial ecosystems have  
856 predominantly focused on its storage and transport within the top 1 m of the soil, which  
857 is usually defined as the biologically active soil zone (or the root zone) in agricultural  
858 ecosystems (Walvoord et al., 2003). In some of the deepest soil boreholes ever taken  
859 from the land surface down to bedrock (56–205 m) at five sites from south to north of  
860 the CLP, we found that a substantial amount of N in deep soils was overlooked due to  
861 the limitation of sampling depth. The stock of mineral N measured by deep sampling  
862 (50–200 m) at the CLP CZO amounted to 0.2–1.0 Pg (Jia et al., 2018), which can  
863 potentially influence the groundwater quality, especially under agricultural land uses  
864 (Turkeltaub et al., 2018). To characterize nitrate accumulation in deep soils and trace  
865 the sources of nitrate in soils and groundwater in the highly-disturbed loess CZ, an  
866 extensive set of groundwater and soil samples from cropland and orchard areas were  
867 collected in the GP. The average amounts of accumulated nitrate in the 0–10 m soil  
868 profile of the orchards were observed to be approximately 3.7 times higher than those  
869 in the same layers of the croplands, suggesting that the cropland-to-orchard transition  
870 aggravated nitrate accumulation in deep soils (Niu et al., 2022). Over 38% of the  
871 groundwater samples had nitrate concentrations exceeding the WHO permissible  
872 standard for drinking (10 mg N L<sup>-1</sup>). Analyses of groundwater  $\delta^{15}\text{N}$  and  $\delta^{18}\text{O}$  of nitrate  
873 indicated that manure and sewage N have been the largest contributors to groundwater  
874 nitrate, followed by soil N and chemical N-fertilizer (Niu et al., 2022). However, in  
875 some areas with thin VZs, the contribution of manure and chemical fertilizers to  
876 groundwater nitrate was comparable (Gao et al., 2021b; Niu et al., 2022).

877 The time lag or residence time of nitrate in the VZ has been estimated using the  
878 chloride mass balance method (Niu et al., 2022) and process-based models (Turkeltaub  
879 et al., 2018). Results indicate that the time required for nitrate to enter the water table  
880 ranges from decades to centuries over the GP. Results of the residence time and source  
881 apportionment suggested that chemical N-fertilizer applied since the 1980s has not  
882 become the dominant source of groundwater nitrate in the entire GP due to the low  
883 recharge rate and thick VZ. However, in Europe and parts of the US and Canada, some  
884 peaks in nitrate in groundwater following intensive post World War II agriculture have

885 been observed (Spalding et al., 1982; Egboka, 1984; Power and Schepers, 1989; Nixon  
886 et al., 2003). It appears that in some parts of the world (e.g., CLP) such peaks are yet to  
887 be observed due to more recent intensive use of N-fertilizers, deep VZ, and slow  
888 transport. Whereas nitrate has already entered the water table in some areas with a  
889 shallow groundwater table in the GP. Unlike the south region of the CLP, groundwater  
890 nitrate contamination in the central part of the region may not be a problem in the near  
891 future due to the thick VZ (>100 m) (Huang et al., 2018; Turkeltaub et al., 2018).  
892 However, the degradation of groundwater quality in the long term appears to be  
893 inevitable.

894 In summary, agricultural land-use changes from cropland to orchards can result in  
895 a relatively high N surplus in deep soils and increase the risk of groundwater nitrate  
896 pollution in the future. The widespread conversion of croplands to orchards on the CLP  
897 should thus be cautiously approached, particularly in areas with shallow VZ and coarse  
898 soil texture. In the short term, a thick VZ increases the time needed for nitrate to reach  
899 the aquifer. However, even with a thick VZ, future generations will suffer from nitrate  
900 in groundwater due to management practices. Thus, it is important to understand both  
901 short-term and long-term consequences and mitigation procedures. Therefore, it is  
902 necessary to modify agricultural production methods (e.g., optimizing fertilization and  
903 irrigation strategies and developing smart water-saving technologies) to achieve a  
904 compromise between the ecological environment and economic development in  
905 cultivated areas with a high risk of groundwater pollution.

#### 906 **4.8. Does Deep Loess Soil Sequester C from the Atmosphere?**

907 Investigating organic C in the Earth's CZ and its response to land-use change is  
908 crucial for understanding the biogeochemical cycling of C and its interaction with the  
909 environment (Marin-Spiotta et al., 2014; Jia et al., 2020). Over the past few decades,  
910 various CLP conservation and restoration strategies have reduced soil erosion and  
911 flooding and enhanced C sequestration and habitat *supporting services* (Jia et al., 2011;  
912 Fu et al., 2017). A regional-scale investigation of vegetation productivity changes from  
913 2000 to 2010 revealed an annual vegetation C sequestration rate of  $9.3 \pm 1.3 \text{ g C m}^{-2} \text{ yr}^{-1}$

914 <sup>1</sup> on the CLP (Feng et al., 2016). This increase in primary production *supporting*  
915 *services* contributes to the CZ's bioenergy production or other forms of production to  
916 support life (Field et al., 2015).

917 Organic C in deep soils greatly contributes to the total C stock and is thus a vital  
918 part of terrestrial C cycles (Rumpel and Kögel-Knabner, 2011; Harper and Tibbett,  
919 2013). Several studies have explored soil organic C stock at various depths in the loess  
920 CZs, such as 2 m (Liu et al., 2011), 5 m (Wang et al., 2016b; Jia et al., 2017c), 18 m  
921 (Gao et al., 2017), 21 m (Wang et al., 2015b), 25.2 m (Li et al., 2019b), and 56–205 m  
922 (Jia et al., 2020). Previous studies limited to shallow soils showed that total organic C  
923 in the 0–2 m loess layer was 5.85 Pg across the entire CLP (Liu et al., 2011).  
924 Calculations from the deepest soil boreholes demonstrated that organic C stored in the  
925 0–100 m loess profile, the mean loess thickness on CLP, amounted to 10.06 Pg for the  
926 entire CLP region (Jia et al., 2020). These studies indicate the high soil organic C  
927 sequestration capacity of deep soil layers. Furthermore, paleosol (generally developed  
928 in a period of warmth and wetness), which is buried at various depths below the loess,  
929 may have high levels of organic C. Marin-Spiotta et al. (2014) found that the Brady soil  
930 (one paleosol), which is buried under 6 meters of loess in southwestern Nebraska, USA,  
931 stores large amounts of organic C. The enrichment of organic C in a buried paleosol  
932 could be explained by an abrupt change in climate, fire, and the loss of vegetative cover  
933 during its exposure and pedogenesis (Marin-Spiotta et al., 2014). The accumulation of  
934 buried organic C in loess-paleosol sequences thus proves the importance of feedback  
935 between climate and the land C sink at geologic and contemporary timescales (Arbogast,  
936 1996; Zech, 2012).

937 Intensive vegetation-restoration activities could significantly influence the  
938 magnitude and distribution of organic C content and stock in deep soil profiles. Net soil  
939 C sequestration in both shallow and deep soil layers has been observed after farmland  
940 conversion in the loess CZ (Wang et al., 2015b). Deng et al. (2014) showed that soil C  
941 sequestration potentials in the 0–20 cm soil layer across the CLP could reach 0.59 Tg  
942 yr<sup>-1</sup> following farmland conversion. Lan et al. (2021) demonstrated that soil organic C  
943 storage in artificial forests increased by 0.9–6.33 kg m<sup>-2</sup> compared to farmland in the



944 20 m soil profile of the semi-arid loess hilly area. [Li et al., \(2019b\)](#) note that while  
945 afforestation of long-term farmland with apple orchards (roots deeper than 20 m) did  
946 not appear to significantly alter soil organic C of the deep soil, it still contributed  $0.44$   
947  $\pm 0.15$  Mg C ha<sup>-1</sup> yr<sup>-1</sup> to the deep soil via root biomass. Notably, vegetation type, soil  
948 depth, and precipitation significantly affect the soil organic C sequestration effect.  
949 [Wang et al. \(2023b\)](#) indicate that woodland had the highest organic C sequestration in  
950 deep soils, while grassland had the lowest on the semi-arid CLP. Soil organic C  
951 sequestration primarily occurred from 2 to 10 m under woodland, 2–6 m under  
952 shrubland, and 2–4 m under grassland. In addition, deep soil organic C sequestration in  
953 woodland significantly decreased as precipitation increased, but no significant  
954 relationship occurred for shrubland and grassland.

955 The vegetation-restoration induced C sequestration in deep soils of the loess CZ is  
956 mainly attributed to the roots C inputs. Perennial grass and forest species on the CLP  
957 can extend their roots deeper than 10 m ([Li et al., 2019c](#); [Wang et al., 2021a](#)). Large  
958 amounts of organic C are released into the soil via root exudation, mycorrhizal  
959 associations, and fine root mortality ([Germon et al., 2020](#); [Panchal et al., 2022](#)). These  
960 processes not only significantly altered deep soil microbes' composition, activities, and  
961 functionality, but also combined with soil physical and chemical properties changes  
962 significantly modifying deep soil C cycling. For instance, the microbial biomass is  
963 much lower in deep soil layers than in the topsoil, which, in combination with oxygen  
964 limitations, could decrease the mineralization rate and hence enhance organic C  
965 sequestration ([Rumpel and Kögel-Knabner, 2011](#); [Marin-Spiotta et al., 2014](#); [Kong et](#)  
966 [al., 2022](#)). Therefore, the interactions among C cycling, land-use change, roots,  
967 microbes, and soil environments along the deep soil profile should be a new focus of  
968 the loess CZ science and should be included in the framework of the loess CZ  
969 observations.

970 In summary, with large-scale vegetation restoration, deep loess soil can potentially  
971 sequester C from the atmosphere via enhancing organic C content or root biomass, of  
972 which degree depends on climatic conditions and vegetation type. Soil C, root biomass,  
973 and exudates in deep soils should be considered when evaluating terrestrial C cycling

974 and soil C sequestration potentials in the loess CZ and similar regions worldwide in the  
975 future.

## 976 **5. New Insights on How Loess CZs Can Achieve SDGs**

977 Severe soil erosion, water shortage, ecosystem degradation, environmental  
978 pollution, and high pressures from human activities are the main socio-ecological  
979 problems for the Earth's loess CZs. Conventional field sampling approaches and  
980 assessments often fail to account for the subsurface's role in CZs with thick loess  
981 deposits. Subsurface influences on loess CZ services (the benefits that loess CZ provide  
982 to the biosphere) have often been ignored or oversimplified in regional assessments and  
983 local planning studies. Therefore, it is important that optimal management interventions  
984 are developed to solve the main socio-ecological problems by considering the CZ  
985 framework. Given the critical role of soil and water in achieving SDGs of the loess CZs,  
986 it is imperative to strengthen our understanding of the relationships between soil and  
987 water processes and agro-ecosystem services, such as grain production, net primary  
988 productivity, C sequestration, water retention, and soil erosion control. The current  
989 understanding of soil and water processes in loess CZs, particularly in the CLP, can  
990 provide some important new insights into achieving SDGs.

991 When linking CZ services with SDGs, three important parts, i.e., agricultural  
992 production, ecological restoration, and environmental protection, should be carefully  
993 considered in loess CZs, given their fragile environments and the great pressure to  
994 sustain large populations. For example, the promotion of agricultural production by  
995 expanding the planting area and intensive use of chemical fertilizers helps to increase  
996 farmer income and alleviate rural poverty (SDGs 1, 2, 3); however, agricultural  
997 intensification has incurred clear eco-environmental trade-offs in terms of high soil  
998 erodibility (SDG 15), severe residual nitrate pollution (SDG 6), and low soil organic C  
999 sequestration (SDG 13). As to ecological restoration, revegetation helps to alleviate soil  
1000 erosion and promote sequestration of more above- and below-ground C, whereas  
1001 extensive planting of exotic deep-rooted species has led to severe deep soil desiccation  
1002 and reduced groundwater recharge (SDG 6). Sustainable solutions to these problems

1003 are essential to improve the delivery of environmental and human-centered SDGs (Fig.  
1004 2). Knowledge from loess CZOs informs us about the critical soil and water processes  
1005 controlling CZ functions and services. Notably, we focused on the CLP as an example  
1006 but many (perhaps not all) of the issues we raised are also relevant to other loess CZs.  
1007 The following are new insights into how critical processes respond to anthropogenic  
1008 changes and how to sustain regional SDGs:

1009 (1) Large-scale vegetation restoration of farmland has reduced soil erosion, but  
1010 further revegetation may exacerbate deficits in the local food supply because of  
1011 diminished farmland. Engineering measures such as building check-dams in channels  
1012 and constructing terraces on hillslopes have been widely used as powerful ecological  
1013 restoration tools to enhance soil and water conservation, gully rehabilitation, and  
1014 hydrological regulation. Terraces and check dam sediments often form fertile  
1015 agricultural lands, with abundant nutrients and water (Wen and Zhen, 2020; Wei et al.,  
1016 2021; Liu et al., 2023b), promoting crop production and supporting livestock. Therefore,  
1017 construction and sustainable management of such engineering measures are effective  
1018 ways not only to conserve soil and water but also to increase grain production, thus,  
1019 achieving a win-win situation on Grain and Green on loess CZs.

1020 (2) Intensive vegetation restoration enhances deep soil C sequestration while  
1021 aggravating water shortages and resulting in deep soil desiccation due to overplanting.  
1022 The trade-offs between C sequestration and water consumption for various vegetation  
1023 types are thus critical for the sustainability of loess ecosystems because most loess CZs  
1024 are limited by water resources (Feng et al., 2017; Li et al., 2018b, 2023a). Future  
1025 vegetation restoration planning should carefully consider the maximum vegetation  
1026 productivity capacity (i.e., the revegetation threshold) supported by local water  
1027 resources. Additionally, vegetation management needs to focus on reducing the uptake  
1028 of (often) limited soil water by vegetation, including plant removal by thinning in high  
1029 plant density areas, and substituting water use efficient native species for water  
1030 depleting species. Furthermore, slope engineering measures (e.g., fish scale pits and  
1031 infiltration holes) can also be useful for deep desiccated soil restoration. Such  
1032 management practices can contribute to the protection and sustainable use of limited

1033 water resources in loess CZs.

1034 (3) The fluxes and mechanisms of GR in loess CZs remain highly uncertain due to  
1035 the thick VZ and complex geomorphic landscapes. However, multiple tracers and  
1036 model simulations have emphasized the importance of preferential or piston-like flow.  
1037 In addition, water stores in weathered bedrock plays an essential role in shaping  
1038 ecohydrological functions, which should not be ignored in the earth system model. New  
1039 monitoring and measurement methods must be developed in the loess CZs, such as  
1040 hydro-geophysical tools, tracer-based techniques, groundwater dating techniques, and  
1041 automatic monitoring equipment. *In situ* observations of water movement and exchange  
1042 processes should be further deployed within the entire loess profile from the surface to  
1043 the groundwater or the weathered bedrock. This information is essential to fully  
1044 understand hydrological processes and evaluate groundwater quantity and quality in the  
1045 loess CZs, providing a reference for sustainable water resource management in other  
1046 loess regions of the world.

1047 (4) The risk of groundwater nitrate pollution is increasing due to a high N surplus  
1048 in deep soils. Although a thick VZ can delay the movement of nitrate to the aquifer, and  
1049 groundwater nitrate contamination in areas with thick VZs may not be a problem in the  
1050 near future, this issue must not be neglected because of the large nitrate accumulation  
1051 in deep soils. Additionally, future agricultural land-use transitions from croplands to  
1052 orchards are cautioned against in areas with shallow VZs and coarse soil texture. Given  
1053 that groundwater is the only source of water for the people and industries situated in  
1054 most loess CZs, farmers in the region should receive guidance to enable them to make  
1055 informed decisions about adopting optimal agricultural management practices, thereby  
1056 increasing their income without compromising future eco-environmental quality.

## 1057 **6. Recommendations for Future CZ Study**

1058 The above new insights provide useful information for local and central  
1059 governments to implement large-scale ecological projects and agricultural management  
1060 practices, achieve harmonious development between society and the environment and  
1061 sustain SDGs. However, one challenge to realizing regional SDGs is the comprehensive

1062 understanding of CZ processes and services, hindered by the lack of long-term  
1063 observations of subsurface processes and the integration of CZ science outcomes across  
1064 scales. Another challenge to the application of CZ knowledge is a scarcity of well-  
1065 trained specialists with a deep knowledge of CZ science. A major concern that some  
1066 CZ scientists have expressed is the lack of a holistic disciplinary foundation to support  
1067 those engaged in CZ science or related activities directly relevant to achieving SDGs.  
1068 Based on our knowledge and experience from the CLP CZOs, we make the following  
1069 recommendations for future CZ studies.

1070 (1) *Strengthen subsurface process observations and use models to help design*  
1071 *future CZ studies.* The findings from the CLP CZOs have demonstrated that subsurface  
1072 processes are important for delivering CZ services, such as grain production, water  
1073 supply, water quality, and C sequestration. While significant progress and  
1074 breakthroughs have been achieved via loess CZ research, quantifying subsurface roles  
1075 in the CZ remains challenging for several reasons: nonlinear physical and  
1076 biogeochemical processes dominate behaviour; heterogeneous soils and weathered  
1077 bedrock cause additional variability; and obtaining high-resolution images or samples  
1078 of these belowground processes and properties proves difficult (Zhu et al., 2018;  
1079 [Dennedy-Frank, 2019](#); [Vereecken et al., 2022](#)). Observation and modeling of hydro-  
1080 biogeochemical processes (e.g., water, nutrients, carbon, and microbial activities) in  
1081 thick soils or sediments from surface to bedrock is recommended for future CZ studies  
1082 to provide comprehensive valuation of CZ services that benefit the sustainable  
1083 development of both the eco-environment and social needs. Future studies will require  
1084 multidisciplinary collaborations and the use of multiple observation and analytical  
1085 techniques to develop an extensive database that is useful for resolving the bottlenecks  
1086 in the coupling interactions of CZ surface and subsurface processes and functions.

1087 (2) *Integrate a series of monitoring sites to guide future regional CZ research.* The  
1088 CLP CZO comprises a series of monitoring sites rather than a single observatory sub-  
1089 catchment. The network covers a distinct gradient in geomorphologic landscape,  
1090 climate, human activities, and social context across the CLP. Multi-catchment  
1091 approaches facilitate a regional understanding of CZ processes and services that

1092 encompass spatial variations in landscape properties, land management, and social-  
1093 economic conditions (Luo et al., 2019). We recommend integrating multiple monitoring  
1094 sites and outcomes (including data, knowledge, and evidence-based management  
1095 measures) to gain a sufficiently comprehensive understanding of CZ processes and  
1096 responses at scales appropriate to local, regional, and national contexts. Scientists, CZ  
1097 residents, and land managers should be involved in data gathering, review, and  
1098 implementation of management change and monitoring to develop strategies to support  
1099 ecosystem function and regeneration across scales, while providing roadmaps for  
1100 sustainable economic development (Naylor et al., 2023).

1101 (3) *Translate CZ science into action through innovative options.* Effective  
1102 communication of the SDGs to societal leaders requires a basic grounding in CZ science  
1103 to enable the public to understand the importance of the Earth's CZ in human lives. This  
1104 includes understanding how soil and water in the CZ are sustained, vary across the  
1105 landscape, and relate to fundamental aspects of the regional economy, such as  
1106 agriculture, forestry, livestock, ecology, and conservation. To bridge the gap between  
1107 researchers, policymakers, farmers, and land managers, and to achieve SDGs, there is  
1108 a strong need to translate CZ science into action through innovative options (Naylor et  
1109 al., 2023). For instance, farmers in the area should receive guidance, enabling them to  
1110 make informed decisions to adopt optimal agricultural and water management practices,  
1111 thus increasing income by maintaining or increasing agricultural production. The loss  
1112 of the benefits from sloping land farming after vegetation restoration can bring about  
1113 significant gains in CZ services such as soil conservation and C sequestration that are  
1114 more valuable on a monetary scale than the crop production, and there will be  
1115 opportunities for compensation from payment schemes for CZ services (Richardson  
1116 and Kumar, 2017). The local farmers and the public may be more motivated to engage  
1117 in environmentally friendly natural resource use activities, which conforms to the  
1118 national strategy for developing an ecological civilization on the plateau.

1119 (4) *Exchange CZ knowledge across sectors and countries.* Policy  
1120 recommendations on soil and water conservation, vegetation restoration, and poverty  
1121 alleviation for CZ services based on scientific evidence from CZ research must be

1122 presented to policymakers in a timely manner. Modern means of communication (e.g.,  
1123 online connectivity and social media) could be explored to reach stakeholders,  
1124 practitioners, and policy makers (e.g., local environmental protection department and  
1125 agricultural management department) designing policies to improve decision-making  
1126 effectiveness on CZ service-related issues. Scientific findings from CZ research should  
1127 also be transferable regionally, nationally, and internationally to ensure sustainable  
1128 provision of CZ services in terrestrial CZ environments where soil degradation, water  
1129 shortage, climate warming, and human perturbation problems are prevalent and where  
1130 these issues have consequences for rural poverty and the human-environment  
1131 relationship. We thus call for international collaborations with multidisciplinary efforts  
1132 to address these issues. These efforts should involve sharing background information  
1133 about the nature and value of loess CZs, including their cultural and economic  
1134 importance, geological formation and evolution, soil properties, water features, erosion,  
1135 degradation, pollution, and restoration and protection efforts and techniques. It is  
1136 important to identify the key scientific challenges of loess CZs worldwide, including  
1137 the current state of knowledge, results of past and planned research, and ongoing  
1138 research needs, with a special emphasis on possible solutions from ecological, social,  
1139 and economic perspectives.

#### 1140 **Acknowledgments**

1141 This study was supported by the National Natural Science Foundation of China  
1142 (42022048), the Strategic Priority Research Program of Chinese Academy of Sciences  
1143 (XDB400200000), the UK Natural Environment Research Council (NE/N007409/1 and  
1144 NE/S009159/1), and USDA-NIFA Multi-State Project 4188. The authors are grateful to  
1145 the editors and reviewers for the thoughtful comments and suggestions towards  
1146 substantially improving the quality of this paper.

#### 1147 **Conflict of Interest**

1148 The authors declare no conflicts of interest relevant to this study.

1149 **References**

- 1150 Arbogast, A.F., 1996. Stratigraphic evidence for late-Holocene aeolian sand mobilization and soil  
1151 formation in south-central Kansas, USA. *J. Arid Environ.* 34, 403–414.  
1152 <https://doi.org/10.1006/jare.1996.0120>.
- 1153 Ascott, M.J., Wang, L., Stuart, M.E., Ward, R.S., Hart, A., 2016. Quantification of nitrate storage in  
1154 the vadose (unsaturated) zone: a missing component of terrestrial N budgets. *Hydrol. Process.* 30,  
1155 1903–1915. <https://doi.org/10.1002/hyp.10748>.
- 1156 Ascott, M.J., Goody, D.C., Wang, L., Stuart, M.E., Lewis, M.A., Ward, R.S., Binley, A.M., 2017.  
1157 Global patterns of nitrate storage in the vadose zone. *Nat. Commun.* 8, 1416.  
1158 <https://doi.org/10.1038/s41467-017-01321-w>.
- 1159 Bai, X., Jia, X.X., Zhao, C.L., Shao, M.A., 2021. Artificial forest conversion into grassland  
1160 alleviates deep-soil desiccation in typical grass zone on China's Loess Plateau: Regional  
1161 modeling. *Agric. Ecosyst. Environ.* 320, 107608. <https://doi.org/10.1016/j.agee.2021.107608>.
- 1162 Bai, X., Shao, M.A., Jia, X.X., and Zhao, C.L., 2022. Prediction of the van Genuchten model soil  
1163 hydraulic parameters for the 5-m soil profile in China's Loess Plateau. *Catena* 210, 105889.  
1164 <https://doi.org/10.1016/j.catena.2021.105889>.
- 1165 Banks, E.W., et al., 2009. Fractured bedrock and saprolite hydrogeologic controls on  
1166 groundwater/surface-water interaction: A conceptual model (Australia). *Hydrogeol J* 17, 1969–  
1167 1989.
- 1168 Banwart, S.A., Nikolaidis, N.P., Zhu, Y.G., Peacock, C.L., Sparks, D.L., 2019. Soil Functions:  
1169 Connecting Earth's Critical Zone. *Annu. Rev. Earth Planet. Sci.* 47, 333–359.  
1170 <https://doi.org/10.1146/annurev-earth-063016-020544>.
- 1171 Baran, N., Richert, J., Mouvet, C., 2007. Field data and modelling of water and nitrate movement  
1172 through deep unsaturated loess. *J. Hydrol.* 345, 27–37.  
1173 <https://doi.org/10.1016/j.jhydrol.2007.07.006>.
- 1174 Bellwood, P.S., 2005. *First Farmers: The Origins of Agricultural Societies*. Blackwell Pub, Malden,  
1175 MA.
- 1176 Bettis III, E.A., Muhs, D.R., Roberts, H.M., & Wintle, A.G., 2003. Last glacial loess in the  
1177 conterminous USA. *Quat. Sci. Rev.* 22, 1907–1946. [https://doi.org/10.1016/S0277-3791\(03\)00169-0](https://doi.org/10.1016/S0277-3791(03)00169-0).
- 1179 Blöschl, G., and other 229 authors, 2019. Twenty-three Unsolved Problems in Hydrology (UPH) –  
1180 a community perspective. *Hydrol. Sci. J.* 64, 1141–1158.  
1181 <https://doi.org/10.1080/02626667.2019.1620507>.
- 1182 Boardman, J., Hazelden, J., 1986. Examples of erosion on brickearth soils in east Kent. *Soil Use*  
1183 *Manage.* 2(3), 105–108. <https://doi.org/10.1111/j.1475-2743.1986.tb00691.x>.
- 1184 Boardman, J., Ligneau, L., De, R.A., Vandaele, K., 1994. Flooding of property by runoff from  
1185 agricultural land in northwestern Europe. *Geomorphology* 10, 183–196.  
1186 <https://doi.org/10.1016/B978-0-444-82012-9.50017-7>.
- 1187 Boardman, J., Evans, R., Ford, J., 2003. Muddy floods on the South Downs, southern England:  
1188 problem and responses. *Environ. Sci. Policy* 6, 69–83. [https://doi.org/10.1016/S1462-9011\(02\)00125-9](https://doi.org/10.1016/S1462-9011(02)00125-9).
- 1190 Cao, R.X., Jia, X.X., Huang, L.M., Zhu, Y.J., Wu, L.H., Shao, M.A., 2018. Deep soil water storage  
1191 varies with vegetation type and rainfall amount in the Loess Plateau of China. *Sci. Rep.* 8, 12346.



1192 <https://doi.org/10.1038/s41598-018-30850-7>.

1193 Cao, X.H., Zheng, Y.J., Lei, Q.L., Li, W.P., Song, S., Wang, C.C., Liu, Y., Khan, K., 2023. Increasing  
1194 actual evapotranspiration on the Loess Plateau of China: An insight from anthropologic activities  
1195 and climate change. *Ecol. Indic.* 157, 111235. <https://doi.org/10.1016/j.ecolind.2023.111235>.

1196 Catt, J.A., 2001. The agricultural importance of loess. *Earth-Sci. Rev.* 54, 213–229.  
1197 [https://doi.org/10.1016/S0012-8252\(01\)00049-6](https://doi.org/10.1016/S0012-8252(01)00049-6).

1198 Chen, Y.Z., Syvitski, J.P.M., Gao, S., Overeem, I., Kettner, A.J., 2012. Socio-economic impacts on  
1199 flooding: A 4000-year history of the Yellow River, China. *Ambio* 41, 682–698.  
1200 <https://doi.org/10.1007/s13280-012-0290-5>.

1201 Chen, Y.P., Wang, K.B., Lin, Y.S., Shi, W.Y., Song, Y., He, X. H., 2015. Balancing green and grain  
1202 trade. *Nature Geosci.* 8(10), 739–741. <https://doi.org/10.1038/ngeo2544>

1203 Chen, Z.J., Wang, L., Wei, A.S., Gao, J.B., Lu, Y.L., Zhou, J.B., 2019. Land-use change from arable  
1204 lands to orchards reduced soil erosion and increased nutrient loss in a small catchment. *Sci. Total*  
1205 *Environ.* 648, 1097–1104. <https://doi.org/10.1016/j.scitotenv.2018.08.141>.

1206 Chen, P.Y., Ma, J.Z., Ma, X.Y., Yu, Q., Cui, X.K., Guo, J.B., 2023. Groundwater recharge in typical  
1207 geomorphic landscapes and different land use types on the Loess Plateau, China. *Hydrol. Process.*  
1208 37, e14860. <https://doi.org/10.1002/hyp.14860>.

1209 Cheng, X.R., Huang, M.B., Shao, M.A., Warrington, D.N., 2009. A comparison of fine roots  
1210 distribution and water consumption of mature *Caragana korshinskii* Kom grown in two soils of  
1211 the semiarid region, China. *Plant Soil* 315, 149–161. <https://doi.org/10.1007/s11104-008-9739-5>.

1212 Chorover, J., Kretzschmar, R., Garcia-Pichel, F., Sparks, D.L., 2007. Soil biogeochemical processes  
1213 in the critical zone. *Elements* 3, 321–326. <https://doi.org/10.2113/gselements.3.5.321>.

1214 Ciampalini, R., Constantine, J.A., Walker-Springett, K.J., Hales, T.C., Ormerod, S.J., Hall, I.R.,  
1215 2020. Modelling soil erosion responses to climate change in three catchments of Great Plain. *Sci*  
1216 *Total Environ.* 749, 141657. <https://doi.org/10.1016/j.scitotenv.2020.141657>.

1217 Dafny, E., Šimůnek, J., 2016. Infiltration in layered loessial deposits: Revised numerical simulations  
1218 and recharge assessment. *J Hydrol.* 538, 339–354. <https://doi.org/10.1016/j.jhydrol.2016.04.029>.

1219 Delmas, M., Pak, L.T., Cerdan, O., Souchère, V., Le Bissonnais, Y., Couturier, A., Sorel, L., 2012.  
1220 Erosion and sediment budget across scale: A case study in a catchment of the European loess belt.  
1221 *J Hydrol.* 420, 255–263. <https://doi.org/10.1016/j.jhydrol.2011.12.008>.

1222 Deng, L., Liu, G.B., Shangguan, Z.P., 2014. Land use conversion and changing soil carbon stocks  
1223 in China's 'Grain-for-Green' Program: a synthesis. *Glob. Change Biol.* 20, 3544–3556.  
1224 <https://doi.org/10.1111/gcb.12508>.

1225 Denny-Frank, P.J., 2019. Including the subsurface in ecosystem services. *Nat. Sustain.* 2, 443–  
1226 444. <https://doi.org/10.1038/s41893-019-0312-4>.

1227 Dotterweich, M., 2013. The history of human-induced soil erosion: Geomorphic legacies, early  
1228 descriptions and research, and the development of soil conservation—A global synopsis.  
1229 *Geomorphology* 201, 1–34. <http://dx.doi.org/10.1016/j.geomorph.2013.07.021>.

1230 Doulabian, S., Toosi, A.S., Calbimonte, G.H., Tousi, E.G., Alaghmand, S., 2021. Projected climate  
1231 change impacts on soil erosion over Iran. *J Hydrol.* 598, 126432.  
1232 <http://dx.doi.org/10.1016/j.jhydrol.2021.126432>.

1233 Eagleson, P.S., 2002. *Ecology: Darwinian Expression of Vegetation Form and Function*.  
1234 Cambridge University Press, Cambridge.

1235 Egboka, B.C.E., 1984. Nitrate contamination of shallow groundwaters in Ontario, Canada. *Sci Total*

1236 Environ. 35(1), 53–70. [https://doi.org/10.1016/0048-9697\(84\)90368-1](https://doi.org/10.1016/0048-9697(84)90368-1).

1237 Enenkel, M., See, L., Bonifacio, R., Boken, V., N. Chaney, N., Vinck, P. You, L.Z., Dutra, E.,  
1238 Anderson, M., 2015. Drought and food security – Improving decision-support via new  
1239 technologies and innovative collaboration. *Glob. Food Secur.* 4, 51–55.  
1240 <https://doi.org/10.1016/j.gfs.2014.08.005>.

1241 Evrard, O., Vandaele, K., Biielders, C., Wesemael, B.V., 2008. Seasonal evolution of runoff  
1242 generation on agricultural land in the Belgian loess belt and implications for muddy flood  
1243 triggering. *Earth Surf. Process. Landforms* 33, 1285–1301. <https://doi.org/10.1002/esp.1613>.

1244 Fang, X.N., Zhao, W.W., Wang, L.X., Feng, Q., Ding, J.Y., Liu, Y.X., Zhang, X., 2016. Variations  
1245 of deep soil moisture under different vegetation types and influencing factors in a watershed of  
1246 the Loess Plateau, China. *Hydrol. Earth Syst. Sci* 20(8), 3309–3323. <https://doi.org/10.5194/hess-20-3309-2016>.

1248 Feng, X.M., Fu, B.J., Piao, S.L., Wang, S., Ciais, P., Zeng, Z.Z., Lü, Y.H., Zeng, Y., Li, Y., Jiang,  
1249 X.H., Wu, B.F., 2016. Revegetation in China’s Loess Plateau is approaching sustainable water  
1250 resource limits, *Nat. Clim. Change* 6, 1019-1022. <https://doi.org/10.1038/nclimate3092>.

1251 Feng, Q., Zhao, W.W., Fu, B.J., Ding, J.Y., Wang, S., 2017. Ecosystem service trade-offs and their  
1252 influencing factors: A case study in the Loess Plateau of China. *Sci. Total Environ.* 607-608,  
1253 1250–1263. <http://dx.doi.org/10.1016/j.scitotenv.2017.07.079>.

1254 Feng, L., Zhang, M.S., Jin, Z., Zhang, S.S., Sun, P.P., Gu, T.F., Liu, X.B., Lin, H., An, Z.S., Peng,  
1255 J.B., Guo, L., 2021. The genesis, development, and evolution of original vertical joints in loess.  
1256 *Earth Sci. Rev.* 214, 103526. <https://doi.org/10.1016/j.earscirev.2021.103526>.

1257 Field, J.P., Breshears, D.D., Law, D.J., Villegas, J.C., López-Hoffman, L., Brooks, P.D., Chorover,  
1258 J., Barron-Gafford, J.A., Gallery, R.E., Litvak, M.E., Lybrand, R.E., McIntosh, J.C., Meixner, T.,  
1259 Niu, G.Y., Papuga, S.A., Pelletier, J.D., Rasmussen, C.R., Troch, P.A., 2015. Critical zone services:  
1260 Expanding context, constraints, and currency beyond ecosystem services. *Vadose Zone J.* 14(1),  
1261 1–7. <https://doi.org/10.2136/vzj2014.10.0142>.

1262 Folberth, C., Khabarov, N., Balkovic, J., Skalsky, R., Visconti, P., Ciais, P., Janssens, I.A., Penuelas,  
1263 J., Obersteiner, M., 2020. The global cropland-sparing potential of high-yield farming. *Nat.*  
1264 *Sustain.* 3(4), 281–289. <https://doi.org/10.1038/s41893-020-0505-x>.

1265 Fu, B.J., Wang, S., Liu, Y., Liu, J.B., Liang, W., Miao, C.Y., 2017. Hydrogeomorphic Ecosystem  
1266 Responses to Natural and Anthropogenic Changes in the Loess Plateau of China. *Annu. Rev.*  
1267 *Earth Planet. Sci.* 45, 223–243. <https://doi.org/10.1146/annurev-earth-063016-020552>

1268 Fu, W., Huang, M.B., Gallichand, J., Shao, M.A. 2012. Optimization of plant coverage in relation  
1269 to water balance in the Loess Plateau of China. *Geoderma* 173-174, 134-144.  
1270 <https://doi.org/10.1016/j.geoderma.2011.12.016>.

1271 Fuchs, S., Leuschner, C., Link M. R., Schuldt, B., 2021. Hydraulic variability of three temperate  
1272 broadleaf tree species along a water availability gradient in central Europe. *New Phytol.*, 231(4),  
1273 1387–1400. <https://doi.org/10.1111/nph.17448>.

1274 Gao, H.D., Li, Z.B., Li, P., Ren, Z.P., Jia, L.L., 2016. Soil Erosion and Soil and Water Conservation  
1275 on the Loess Plateau at Multi-scale. Science Press, Beijing (in Chinese).

1276 Gao, L., Shao, M.A., Wang, Y.Q., 2012. Spatial scaling of saturated hydraulic conductivity of soils  
1277 in a small watershed on the Loess Plateau, China. *J. Soils Sediments* 12, 863–875.  
1278 <https://doi.org/10.1007/s11368-012-0511-3>.

1279 Gao, X.D., Meng, T.T., Zhao, X.N., 2017. Variations of soil organic carbon following land use

1280 change on deep-loess hillslopes in China. *Land Degrad. Develop.* 28, 1902–1912.  
1281 <https://doi.org/10.1002/ldr.2693>.

1282 Gao, X.D., Zhao, X.N., Wu, P.T., Yang, M., Ye, M.T., Tian, L., Zou, Y.F., Wu, Y., Zhang, F.S.,  
1283 Siddique K.H.M., 2021a. The economic-environmental trade-off of growing apple trees in the  
1284 drylands of China: A conceptual framework for sustainable intensification. *J. Cleaner Production*  
1285 296, 126497. <http://dx.doi.org/10.1016/j.jclepro.2021.126497>.

1286 Gao, J.B., Wang, S.M., Li, Z.Q., Wang, L., Chen, Z.J., Zhou, J.B., 2021b. High Nitrate Accumulation  
1287 in the Vadose Zone after Land-Use Change from Croplands to Orchards. *Environ. Sci. Technol.*  
1288 55, 5782–5790. <https://doi.org/10.1021/acs.est.0c06730>.

1289 Gao, J.B., Li, Z.Q., Chen, Z.J., Zhou, Y., Liu, W.G., Wang, L., Zhou, J.B., 2021c. Deterioration of  
1290 groundwater quality along an increasing intensive land use pattern in a small catchment. *Agric.*  
1291 *Water Manag.* 253, 106953. <https://doi.org/10.1016/j.agwat.2021.106953>.

1292 Gao, X.D., Wan, H., Zeng, Y.J., Shao, X.Y., Hu, W., Brocca, L., Yang, M., Wu, P.T., Zhao, X.N.,  
1293 2023. Disentangling the Impact of Event- and Annual-Scale Precipitation Extremes on Critical-  
1294 Zone Hydrology in Semiarid Loess Vegetated by Apple Trees. *Water Resour. Res.* 59(3),  
1295 e2022WR033042. <https://doi.org/10.1029/2022WR033042>.

1296 Ge, J., Pitman, A.J., Guo, W.D., Zan, B.L., Fu, C.B., 2020. Impact of revegetation of the Loess  
1297 Plateau of China on the regional growing season water balance. *Hydrol. Earth Syst. Sci.* 24, 515–  
1298 533. <https://doi.org/10.5194/hess-24-515-2020>.

1299 Ge, J.M., Fan, J., Yang, X.T., Luo, Z.B., Zhang, S.G., Yuan, H.Y., 2022. Restoring soil water content  
1300 after alfalfa and Korshinsk peashrub conversion to cropland and grassland. *Hydrol. Process.* 36,  
1301 e14539. <https://doi.org/10.1002/hyp.14539>.

1302 Germon, A., Laclau, J.P., Robin, A., Jourdan, C., 2020. Tamm review: deep fine roots in forest  
1303 ecosystems: why dig deeper. *Forest Ecol. Manag.* 466, 118135.  
1304 <https://doi.org/10.1016/j.foreco.2020.118135>.

1305 Giardino, J.R., Houser, C., 2015. Principles and Dynamics of the Critical Zone. *Developments in*  
1306 *Earth Surface Processes*. Elsevier.

1307 Goulden, M.L., Bales, R.C., 2019. California forest die-off linked to multi-year deep soil drying in  
1308 2012-2015 drought. *Nature Geosci.* 12, 632–637. <https://doi.org/10.1038/s41561-019-03>.

1309 Guo, L., Lin, H., 2016. Critical zone research and observatories: current status and future  
1310 perspectives. *Vadose Zone J.*, 15(9), 1539–1663, <https://doi.org/10.2136/vzj2016.06.0050>.

1311 Guo, T.L., Wang, Q.J., Li, D.Q., Zhuang, J., 2010. Effect of surface stone cover on sediment and  
1312 solute transport on the slope of fallow land in the semi-arid loess region of northwestern China.  
1313 *J. Soils Sediments* 10(6), 1200–1208. <https://doi.org/10.1007/s11368-010-0257-8>.

1314 Gun, L.H., Huang, C. C., Zhou, Z. X., 2007. The Pollution of Underground Water and Its Impact on  
1315 Urban Development in Ancient Xi'an City. *J. Northwest Univ.* 37, 326–329. (In Chinese)  
1316 <https://doi.org/10.16152/j.cnki.xdxbzr.2007.02.038>

1317 Gvirtzman, H., Shalev, E., Dahan, O., Hatzor, Y.H., 2008. Large-scale infiltration experiments into  
1318 unsaturated stratified loess sediments: Monitoring and modeling. *J Hydrol.* 349(1–2), 214–229.  
1319 <https://doi.org/10.1016/j.jhydrol.2007.11.002>.

1320 Hahm, W.J., Dralle, D.N., Sanders, M., Bryk, A.B., Fauria, K.E., Huang, M.H., Hudson-Rasmussen,  
1321 B., Nelson, M.D., Pedrazas, M.A., Schmidt, L., Whiting, J., Dietrich, W.E., Rempe, D.M., 2022.  
1322 Bedrock vadose zone storage dynamics under extreme drought: Consequences for plant water  
1323 availability, recharge, and runoff. *Water Resour. Res.* 58(4)

1324 <https://doi.org/10.1029/2021WR031781>.

1325 Hanson, G.J., Simon, A., 2001. Erodibility of cohesive streambeds in the loess area of the midwestern  
1326 USA. *Hydrol. Process* 15, 23–38. <https://doi.org/10.1002/hyp.149>.

1327 Harper, R.J., Tibbett, M., 2013. The hidden organic carbon in deep mineral soils. *Plant Soil* 368,  
1328 641–648. <https://doi.org/10.1007/s11104-013-1600-9>.

1329 Hasenmueller, E.A., Gu, X., Weitzman, J.N., Adams, T.S., Stinchcomb, G.E., Eissenstat, D.M.,  
1330 Drohan, P.J., Brantley, S.L., Kaye, J.P., 2017. Weathering of rock to regolith: the activity of deep  
1331 roots in bedrock fractures. *Geoderma* 300, 11–31.  
1332 <https://doi.org/10.1016/j.geoderma.2017.03.020>.

1333 He, M.N., Wang, Y.Q., Wang, L., Jia, X.X., Zhao, C.L., Zhang, P.P., 2022. Spatial–temporal  
1334 dynamics and recovery mechanisms of dried soil layers under Robinia pseudoacacia forest based  
1335 on in-situ field data from 2017 to 2020. *Land Degrad. Dev.* 33(14), 2500–2511.  
1336 <https://doi.org/10.1002/ldr.4327>.

1337 He, N.N., Gao, X.D., Guo, D.G., Wu, Y.B., Ge, D., Zhao, L.H., Tian, L., Zhao, X.N., 2023. The  
1338 degree and depth limitation of deep soil desiccation and its impact on xylem hydraulic  
1339 conductivity in dryland tree plantations. *Hydrol. Earth Syst. Sci. Discuss.*  
1340 <https://doi.org/10.5194/hess-2023-12>.

1341 Hou, X.K., Li, T.L., Vanapalli, S.K., Xi, Y., 2018. Water percolation in a thick unsaturated loess  
1342 layer considering the ground-atmosphere interaction. *Hydrol. Process* 33(5), 794–802.  
1343 <https://doi.org/10.1002/hyp.13364>.

1344 Hu, C.H., Zhang, X.M., 2020. Loess Plateau soil erosion governance and runoff-sediment variation  
1345 of Yellow River. *Water Resour. Hydropower Eng.* 51(1), 1–11 (In Chinese).  
1346 <https://doi.org/10.13928/j.cnki.wrahe.2020.01.001>.

1347 Hu, W., Wang, Y.Q., Li, H.J., Huang, M.B., Hou, M.T., Li, Z., She, D.L., Si, B.C., 2019. Dominant  
1348 role of climate in determining spatio-temporal distribution of potential groundwater recharge at a  
1349 regional scale. *J Hydrol.* 578, 124042. <https://doi.org/10.1016/j.jhydrol.2019.124042>.

1350 Huang, M.B., Gallichand, J., 2006. Use of the SHAW model to assess soil water recovery after apple  
1351 trees in the gully region of the Loess Plateau, China. *Agric. Water Manag.* 85, 67–76.  
1352 <https://doi.org/10.1016/j.agwat.2006.03.009>.

1353 Huang, T.M., Pang, Z.H., 2011. Estimating groundwater recharge following land-use change using  
1354 chloride mass balance of soil profiles: a case study at Guyuan and Xifeng in the Loess Plateau of  
1355 China. *Hydrogeol. J.* 19(1), 177–186. <https://doi.org/10.1007/s10040-010-0643-8>.

1356 Huang, T.M., Pang, Z.H., Liu, J.L., Ma, J.Z., Gates, J., 2017. Groundwater recharge mechanism in  
1357 an integrated tableland of the Loess Plateau, northern China: insights from environmental tracers.  
1358 *Hydrogeol. J.* 25(7), 2049–2065. <https://doi.org/10.1007/s10040-017-1599-8>.

1359 Huang, Y.N., Chang, Q.R., Li, Z., 2018. Land use change impacts on the amount and quality of  
1360 recharge water in the loess tablelands of China. *Sci. Total Environ.* 628–629, 443–452.  
1361 <https://doi.org/10.1016/j.scitotenv.2018.02.076>.

1362 Huang, Y.N., Evaristo, J., Li, Z., 2019. Multiple tracers reveal different groundwater recharge  
1363 mechanisms in deep loess deposits. *Geoderma* 353, 204–212.  
1364 <https://doi.org/10.1016/j.geoderma.2019.06.041>.

1365 Huang, T.M., Ma, B., Pang, Z., Li, Z., Li, Z., Long, Y., 2020. How does precipitation recharge  
1366 groundwater in loess aquifers? Evidence from multiple environmental tracers. *J Hydrol.* 583,  
1367 124532. <https://doi.org/10.1016/j.jhydrol.2019.124532>.

1368 Huang, Y.N., Li, B.B., Li, Z., 2021. Conversion of degraded farmlands to orchards decreases  
1369 groundwater recharge rates and nitrate gains in the thick loess deposits. *Agric. Ecosyst. Environ.*  
1370 314, 107410. <https://doi.org/10.1016/j.agee.2021.107410>.

1371 Jia, X.X., Shao, M.A., Wei, X.R., 2011. Richness and composition of herbaceous species in restored  
1372 shrubland and grassland ecosystems in the northern Loess Plateau of China. *Biodivers. Conserv.*  
1373 20, 3435–3452. <http://dx.doi.org/10.1007/s10531-011-0130-0>.

1374 Jia, X.X., Shao, M.A., Wei, X.R., 2012. Responses of soil respiration to N addition, burning and  
1375 clipping in temperate semiarid grassland in northern China. *Agric. For. Meteorol.* 166-167, 32–  
1376 40. <http://dx.doi.org/10.1016/j.agrformet.2012.05.022>.

1377 Jia, X.X., Shao, M.A., Wei, X.R., Wang, Y.Q., 2013. Hillslope scale temporal stability of soil water  
1378 storage in diverse soil layers. *J. Hydrol.* 498, 254–264.  
1379 <http://dx.doi.org/10.1016/j.jhydrol.2013.05.042>.

1380 Jia, X.X., Shao, M.A., Wei, X.R., Li, X.Z., 2014. Response of soil CO<sub>2</sub> efflux to water addition in  
1381 temperate semiarid grassland in northern China: the importance of water availability and species  
1382 composition. *Biol. Fertil. Soils* 50, 839–850. <http://dx.doi.org/10.1007/s00374-014-0901-3>.

1383 Jia, X.X., Shao, M.A., Zhang, C.C., Zhao, C.L., 2015. Regional temporal persistence of dried soil  
1384 layer along south-north transect of the Loess Plateau, China. *J. Hydrol.* 582, 152–160.  
1385 <http://dx.doi.org/10.1016/j.jhydrol.2015.06.025>.

1386 Jia, X.X., Shao, M.A., Zhu, Y.J., Luo, Y., 2017a. Soil moisture decline due to afforestation across  
1387 the Loess Plateau, China. *J. Hydrol.* 546, 113–122.  
1388 <http://dx.doi.org/10.1016/j.jhydrol.2017.01.011>.

1389 Jia, X.X., Wang, Y.Q., Shao, M.A., Luo, Y., Zhang, C., 2017b. Estimating regional losses of soil  
1390 water due to the conversion of agricultural land to forest in China's Loess Plateau. *Ecohydrology*  
1391 10, e1851. <https://doi.org/10.1002/eco.1851>.

1392 Jia, X.X., Yang, Y., Zhang, C.C., Shao, M.A., Huang, L.M., 2017c. A state-space analysis of soil  
1393 organic carbon in China's Loess Plateau. *Land Degrad. Develop.* 28, 983-993.  
1394 <https://doi.org/10.1002/ldr.2675>.

1395 Jia, X.X., Zhu, Y.J., Huang, L.M., Wei, X.R., Fang, Y.T., Wu, L.H., Binley, A., Shao, M.A., 2018.  
1396 Mineral N stock and nitrate accumulation in the 50 to 200 m profile on the Loess Plateau. *Sci.*  
1397 *Total Environ.* 633, 999–1006. <https://doi.org/10.1016/j.scitotenv.2018.03.249>.

1398 Jia, X.X., Shao, M.A., Yu, D.X., Zhang, Y., Binley, A., 2019. Spatial variations in soil-water carrying  
1399 capacity of three typical revegetation species on the Loess Plateau, China. *Agric. Ecosyst.*  
1400 *Environ.* 273, 25–35. <https://doi.org/10.1016/j.agee.2018.12.008>.

1401 Jia, X.X., Wu, H.M., Shao, M.A., Huang, L.M., Wei, X.R., Wang, Y.Q., Zhu, Y.J., 2020. Re-  
1402 evaluation of organic carbon pool from land surface down to bedrock on China's Loess Plateau.  
1403 *Agr. Ecosyst. Environ.* 293, 106842. <https://doi.org/10.1016/j.agee.2020.106842>.

1404 Jian, S.Q., Zhao, C.Y., Fang, S.M., Yu, K., 2014. Distribution of fine root biomass of main planting  
1405 tree species in Loess Plateau, China. *Chin. J. Appl. Ecol.* 25(7), 1905–1911. (In Chinese)  
1406 <http://dx.doi.org/10.13287/j.1001-9332.20140429.004>.

1407 Jiang, Z.H., Liu, H.Y., Wang, H.Y., Peng, J., Meersmans, J., Green, S.M., Quine, T.A., Wu, X.C.,  
1408 Song, Z.L., 2020. Bedrock geochemistry influences vegetation growth by regulating the regolith  
1409 water holding capacity. *Nat. Commun.* 11, 2392. <https://doi.org/10.1038/s41467-020-16156-1>.

1410 Jiménez-Rodríguez, C.D., Sulis, M., Schymanski, S., 2022. Exploring the role of bedrock  
1411 representation on plant transpiration response during dry periods at four forested sites in Europe.

1412 Biogeosciences 19(14), 3395–3423. <https://doi.org/10.5194/bg-19-3395-2022>.

1413 Jin, Z., Cui, B.L., Song, Y., Shi, W.Y., Wang, K.B., Wang, Y., Liang, J., 2012. How many check  
1414 dams do we need to build on the Loess Plateau? *Environ. Sci. Technol.* 46(16), 8527–8528.  
1415 <https://doi.org/10.1021/es302835r>.

1416 Kemp, R.A., 2001. Pedogenic modification of loess: significance for paleoclimatic reconstructions.  
1417 *Earth-Sci. Rev.* 54, 145–156. [https://doi.org/10.1016/S0012-8252\(01\)00045-9](https://doi.org/10.1016/S0012-8252(01)00045-9).

1418 Kervroëdan, L., Armand, R., Saunier, M., Faucon, M.P., 2019. Effects of plant traits and their  
1419 divergence on runoff and sediment retention in herbaceous vegetation. *Plant Soil* 441, 511–524.  
1420 <https://doi.org/10.1007/s11104-019-04142-6>.

1421 Kim, H., Dietrich, W.E., Thurnhoffer, B.M., Bishop, J.K., Fung, I.Y., 2017. Controls on solute  
1422 concentration-discharge relationships revealed by simultaneous hydrochemistry observations of  
1423 hillslope runoff and stream flow: The importance of critical zone structure. *Water Resour. Res.*  
1424 53,1424–1443.

1425 Kong, W.B., Wei, X.R., Wu, Y.H., Shao, M.A., Zhang, Q., Sadowsky, M.J., Ishii, S., Reich, P.B.,  
1426 Wei, G.H., Jiao, S., Qiu, L.P., Liu, L.L., 2022. Afforestation can lower microbial diversity and  
1427 functionality in deep soil layers in a semiarid region, *Global Change Biol.* 00, 1–16.  
1428 <https://onlinelibrary.wiley.com/doi/epdf/10.1111/gcb.16334>.

1429 Kramer, L.A., Burkart, M.R., Meek, D.W., Jaquis, R.J., James, D.E., 1999. Field-scale watershed  
1430 evaluations on deep loess soils. II. Hydrologic responses to different management systems. *J. Soil*  
1431 *Water Conserv.* 54(4), 705–710.

1432 Kremer, R.J., Kussman, R.D., 2011. Soil quality in a pecan-kura clover alley cropping system in the  
1433 Midwestern USA. *Agroforest Syst.* 83, 213–223. <https://doi.org/10.1007/s10457-011-9370-y>.

1434 Lal, R., Bouma, J., Brevik, E., Dawson, L., Field, D., Glaser, B., Hatano, R., Hartemink, A., Kosaki,  
1435 T., Lascelles, B., Monger, C., Ndzana, G.M., Norra, S., Pan, X.C., Paradelo, R., Reyes-Sánchez,  
1436 L.B., Sandén, T., Singh, B.R., Spiegel, H., Zhang, J.B., 2021. Soils and sustainable development  
1437 goals of the United Nations: An International Union of Soil Sciences perspective, *Geoderma* 25,  
1438 e00398. <https://doi.org/10.1016/j.geodrs.2021.e00398>.

1439 Lan, Z., Zhao, Y., Zhang, J., Jiao, R., Khan, M.N., Sial, T.A., Si, B., 2021. Long-term vegetation  
1440 restoration increases deep soil carbon storage in the Northern Loess Plateau. *Sci. Rep.* 11(1),  
1441 13758. <https://doi.org/10.1038/s41598-021-93157-0>.

1442 Lapides, D.A., Hahm, W.J., Forrest, M., Rempe, D.M., Hickler, T., Dralle, D.N., 2024. Inclusion of  
1443 bedrock vadose zone in dynamic global vegetation models is key for simulating vegetation  
1444 structure and function. *Biogeosciences* 21, 1801–1826. <https://doi.org/10.5194/bg-21-1801-2024>.

1445 Li, X.Y., 2000. Soil and water conservation in arid and semiarid area: the Chinese experience. *Ann.*  
1446 *Arid Zone* 39(4), 1–18.

1447 Li, Z., Chen, X., Liu, W.Z., Si, B.C., 2017. Determination of groundwater recharge mechanism in  
1448 the deep loessial unsaturated zone by environmental traces. *Sci. Total Environ.* 586, 827–835.  
1449 <http://dx.doi.org/10.1016/j.scitotenv.2017.02.061>.

1450 Li, H., Si, B.C., Li, M., 2018a. Rooting depth controls potential groundwater recharge on hillslopes.  
1451 *J Hydrol.* 564, 164–174. <https://doi.org/10.1016/j.jhydrol.2018.07.002>.

1452 Li, B.Y., Chen, N.C., Wang, Y.C., Wang, W., 2018b. Spatio-temporal quantification of the trade-offs  
1453 and synergies among ecosystem services based on grid-cells: A case study of Guanzhong Basin,  
1454 NW China, *Ecol. Indic.* 94, 246–253. <https://doi.org/10.1016/j.ecolind.2018.06.069>.

1455 Li, Z., Jasechko, S., Si, B.C., 2019a. Uncertainties in tritium mass balance models for groundwater

1456 recharge estimation, *J Hydrol.* 571, 150–158. <https://doi.org/10.1016/j.jhydrol.2019.01.030>.

1457 Li, H.J., Si, B.C., Ma, X.J., Wu, P.T., 2019b. Deep soil water extraction by apple sequesters organic  
1458 carbon via root biomass rather than altering soil organic carbon content, *Sci. Total Environ.* 670,  
1459 662–671. <https://doi.org/10.1016/j.scitotenv.2019.03.267>.

1460 Li, H.J., Si, B.C., Ma, X.J., Wu, P.T., McDonnell, J.J., 2019c. Water mining from the deep critical  
1461 zone by apple trees growing on loess. *Hydrol. Process.* 33, 320–327.  
1462 <https://doi.org/10.1002/hyp.13346>.

1463 Li, Y.R., Shi, W.H., Aydin, A., Beroya-Eitner, M.A., Gao, G.H., 2020. Loess genesis and worldwide  
1464 distribution. *Earth-Sci. Rev.* 201, 102947. <https://doi.org/10.1016/j.earscirev.2019.102947>.

1465 Li, H.J., Ma, X.J., Lu, Y.W., Ren, R.Q., Cui, B.L., Si, B.C., 2021. Growing deep roots has opposing  
1466 impacts on the transpiration of apple trees planted in subhumid loess region. *Agric. Water Manage.*  
1467 258, 107207. <https://doi.org/10.1016/j.agwat.2021.107207>.

1468 Li, H.J., Li, H., Wu, Q.F., Si, B.C., Jobbágy, E.G., McDonnell, J.J., 2023a. Afforestation triggers  
1469 water mining and a single pulse of water for carbon trade-off in deep soil. *Agri. Ecosyst. Environ.*  
1470 356, 108655. <https://doi.org/10.1016/j.agee.2023.108655>.

1471 Li, Y., Zhang, B.Q., Shao, R., Su, T.X., Wang, X.J., Tian, L., He, C.S., 2023b. Estimating the  
1472 maximum vegetation coverage and productivity capacity supported by rainwater resources on the  
1473 Loess Plateau. *J Hydrol.* 619, 129346. <https://doi.org/10.1016/j.jhydrol.2023.129346>.

1474 Lin, R.F., Wei, K.Q., 2006. Tritium profiles of pore water in the Chinese loess unsaturated zone:  
1475 implications for estimation of groundwater recharge. *J Hydrol.* 328, 192–199.  
1476 <https://doi.org/10.1016/j.jhydrol.2005.12.010>

1477 Lin, H., 2010. Earth's critical zone and hydrogeology: Concepts, characteristics, and advances.  
1478 *Hydrol. Earth Syst. Sci.* 14, 25–45. <https://doi.org/10.5194/hess-14-25-2010>.

1479 Lin, H., Hopmans, J.W., Richter, D.D.B., 2011. Interdisciplinary sciences in a global network of  
1480 critical zone observatories. *Vadose Zone J.* 10(3), 781–785. <https://doi.org/10.2136/vzj2011.0084>.

1481 Liu, T.S., 1985. Loess and the environment. Science Press, Beijing (in Chinese).

1482 Liu, L., 2004. The Chinese Neolithic: Trajectories to Early States. Cambridge University Press,  
1483 Cambridge, UK.

1484 Liu, Z., Shao, M., Wang, Y., 2011. Effect of environmental factors on regional soil organic carbon  
1485 stocks across the Loess Plateau region, China. *Agric. Ecosyst. Environ.* 142, 184–194.  
1486 <https://doi.org/10.1016/j.agee.2011.05.002>

1487 Liu, Q., Wang, Y.Q., Zhang, J., Chen, Y.P., 2013. Filling Gullies to Create Farmland on the Loess  
1488 Plateau. *Environ. Sci. Technol.* 47(14), 7589–7590. <https://doi.org/10.1021/es402460r>

1489 Liu, Q.S., Jin, C.S., Hu, P.X., Jiang, Z.X., Ge, K.P., Roberts, A.P., 2015. Magnetostratigraphy of  
1490 Chinese loess-paleosol sequences. *Earth-Sci. Rev.* 150, 139–167.  
1491 <http://dx.doi.org/10.1016/j.earscirev.2015.07.009>.

1492 Liu, Y., Song, H.M., An, Z.S., Sun, C.F., Trouet, V., Cai, Q.F., Liu, R.S., Leavitt, S.W., Song, Y., Li,  
1493 Q., Fang, C.X., Zhou, W.J., Yang, Y.K., Jin, Z., Wang, Y.Q., Sun, J.Y., Mu, X.M., Lei, Y., Wang,  
1494 L., Li, X.X., Ren, M., Cui, L.L., Zeng, X.L., 2020a. Recent anthropogenic curtailing of Yellow  
1495 River runoff and sediment load is unprecedented over the past 500 y. *Proc. Natl. Acad. Sci.*  
1496 117(31), 18251–18257. <http://dx.doi.org/10.1073/pnas.1922349117>.

1497 Liu, Y., Kumar, M., Katul, G. G., Feng, X., Konings, A. G., 2020b. Plant hydraulics accentuates the  
1498 effect of atmospheric moisture stress on transpiration. *Nat. Clim. Change*, 10(7), 691–695,  
1499 <https://doi.org/10.1038/s41558-020-0781-5>.

1500 Liu, C.G., Jia, X.X., Ren, L.D., Zhu, X.C., Shao, M.A., 2023a. Evaluation of the soil water content  
1501 of two managed ecosystems using cosmic-ray neutron sensing on China's Loess Plateau. *Eur. J.*  
1502 *Soil Sci.* 74, e13339. <https://doi.org/10.1111/ejss.13339>.

1503 Liu, C.G., Jia, X.X., Ren, L.D., Duan, G.X., Shao, M.A., 2023b. A preliminary investigation of  
1504 water storage in check-dams across China's Loess Plateau using electrical resistivity tomography.  
1505 *Hydrol. Process.* 37, e14826. <https://doi.org/10.1002/hyp.14826>.

1506 Lu, Y.W., Li, H.J., Si, B.C., Li, M., 2020. Chloride tracer of the loess unsaturated zone under sub-  
1507 humid region: A potential proxy recording high-resolution hydroclimate. *Sci. Total Environ.* 700,  
1508 134465. <https://doi.org/10.1016/j.scitotenv.2019.134465>.

1509 Lu, Y.L., Zhou, J.B., Sun, L.K., Gao, J.B., Raza, S., 2022. Long-term land-use change from cropland  
1510 to kiwifruit orchard increases nitrogen load to the environment: A substance flow analysis. *Agri.*  
1511 *Ecosyst. Environ.* 335, 108013. <https://doi.org/10.1016/j.agee.2022.108013>.

1512 Lu, D.F., Zheng, Y.J., Cao, X.H., Guan, J.J., Li, W.P., Khan, K., 2024. Dynamic changes in terrestrial  
1513 water balance using remote sensing on the Loess Plateau. *Water* 16, 845.  
1514 <https://doi.org/10.3390/w16060845>.

1515 Luan, J.K., Miao, P., Tian, X.Q., Li, X.J., Ma, N., Faiz, M.A., Xu, Z.W., Zhang, Y.Q., 2022.  
1516 Estimating hydrological consequences of vegetation greening. *J Hydrol.* 611, 128018.  
1517 <https://doi.org/10.1016/j.jhydrol.2022.128018>.

1518 Luo, Y., Lu, Y.H., Fu, B.J., Harris, P., Wu, L.H., Comber, A., 2019. When multi-functional landscape  
1519 meets Critical Zone science: advancing multi-disciplinary research for sustainable human well-  
1520 being, *National Sci. Rev.* 6(2), 349–358. <https://doi.org/10.1093/nsr/nwy003>.

1521 Luo, Z.B., Yong, C.X., Fan, J., Shao, M.A., Wang, S., Jin, M., 2020. Precipitation recharges the  
1522 shallow groundwater of check dams in the loessial hilly and gully region of China. *Sci Total*  
1523 *Environ.* 742, 140625. <https://doi.org/10.1016/j.scitotenv.2020.140625>.

1524 Luo, Z.B., Fan, J., Shao, M.A., Yang, Q., Gan, M., 2023. Weathered bedrock converts hydrological  
1525 processes in loess hilly-gully critical zone. *J Hydrol.* 625, 130112.  
1526 <https://doi.org/10.1016/j.jhydrol.2023.130112>.

1527 Luo, Z.B., Fan, J., Shao, M.A., Yang, Q., Yang, X.T., Zhang, S.G., 2024. Evaluating soil water  
1528 dynamics and vegetation growth characteristics under different soil depths in semiarid loess areas.  
1529 *Geoderma* 442, 116791. <https://doi.org/10.1016/j.geoderma.2024.116791>.

1530 Ma, L.H., Wang, X., Gao, Z.Y., Wang, Y.K., Nie, Z.Y., Liu, X.L., 2019. Canopy pruning as a strategy  
1531 for saving water in a dry land jujube plantation in a loess hilly region of China. *Agric. Water*  
1532 *Manage.* 216, 436–443. <https://doi.org/10.1016/j.agwat.2018.12.007>.

1533 Manna, F., Walton, K.M., Cherry, J.A., Parker, B.L., 2017. Mechanisms of recharge in a fractured  
1534 porous rock aquifer in a semi-arid region, *J. Hydrol.* 555, 869–880.  
1535 <https://doi.org/10.1016/j.jhydrol.2017.10.060>.

1536 Marin-Spiotta, E., Chaopricha, N.T., Plante, A.F., Diefendorf, A.F., Mueller, C.W., Grandy, A.S.,  
1537 Mason, J.A., 2014. Long-term stabilization of deep soil carbon by fire and burial during early  
1538 Holocene climate change. *Nat. Geosci.* 7(6), 428–432. <https://doi.org/10.1038/NGEO2169>.

1539 McCormick, E.L., Dralle, D.N., Hahm, W.J., Tune, A.K., Schmidt, L.M., Chadwick, K.D., Rempe,  
1540 D.M., 2021. Widespread woody plant use of water stored in bedrock. *Nature* 597(7875), 225–229.  
1541 <https://doi.org/10.1038/s41586-021-03761-3>.

1542 Meninno, S., Canelas, R.B., Cardoso, A.H., 2020. Coupling check dams with large wood retention  
1543 structures in clean water. *Environ. Fluid Mech.* 20, 619–634.



1544 09711-y.

1545 Meter, K.J.V., Basu, N.B., Veenstra, J.J., Burras, C.L., 2016. The nitrogen legacy: emerging  
1546 evidence of nitrogen accumulation in anthropogenic landscapes. *Environ. Res. Lett.* 11, 035014.  
1547 <https://doi.org/10.1088/1748-9326/11/3/035014>.

1548 Minor, J., Jessie, K., Mallory, P., Barnes, L., Colella, T.R., Murphy, P.C., Mann, S., Barron-Gafford,  
1549 G.A., 2020. Critical Zone Science in the Anthropocene: Opportunities for biogeographic and  
1550 ecological theory and praxis to drive earth science integration. *Prog. Phys. Geog.* 44(1), 50–69.  
1551 <https://doi.org/10.1177/0309133319864268>.

1552 Moeck, C., Grech-Cumbo, N., Podgorski, J., Bretzler, A., Gurdak, J.J., Berg, M., Schirmer, M., 2023.  
1553 A global-scale dataset of direct natural groundwater recharge rates: A review of variables,  
1554 processes and relationships. *Sci Total Environ.* 717, 137042.  
1555 <https://doi.org/10.1016/j.scitotenv.2020.137042>.

1556 Moorman, T.B., Cambardella, C.A., James, D.E., Karlen, D.L., Kramer, L.A., 2004. Quantification  
1557 of tillage and landscape effects on soil carbon in small Iowa watersheds. *Soil Till. Res.* 78, 225–  
1558 236. <https://doi.org/10.1016/j.still.2004.02.014>.

1559 Morford, S.L., Houlton, B.Z., Dahlgren, R.A., 2011. Increased forest ecosystem carbon and nitrogen  
1560 storage from nitrogen rich bedrock. *Nature* 477, 78–81. <https://doi.org/10.1038/nature10415>.

1561 Mukhopadhyay, K., Thomassin, P. J., Zhang, J., 2018. Food security in China at 2050: A global CGE  
1562 exercise. *J. Eco. Struc.* 7, 1. <https://doi.org/10.1186/s40008-017-0097-4>.

1563 National Research Council, 2001. Basic Research Opportunities in Earth Science, The National  
1564 Academies Press, Washington, D. C.

1565 Naylor, L.A., Dungait, J.A.J., Zheng, Y., Buckerfield, S., Green, S.M., Oliver, D.M., Liu, H.Y., Peng,  
1566 J., Tu, C.L., Zhang, G.L., Zhang, X.Y., Quine, T.A., Waldron, S., Hallett, P.D., 2023. Achieving  
1567 sustainable Earth futures in the Anthropocene by including local communities in critical zone  
1568 science. *Earth Future* 11, e2022EF003448. <https://doi.org/10.1029/2022EF003448>.

1569 NFGA (National Forestry and Grassland Administration of China), 2020. Twenty years of Grain for  
1570 Green in China (1999–2020). Beijing (in Chinese).

1571 Niu, X.Z., Williams, J.Z., Miller, D., Lehnert, K., Bills, B., Brantley, S.L., 2014. An ontology driven  
1572 relational geochemical database for the Earth’s Critical Zone: CZchemDB. *J. Environ. Inform.*  
1573 23(2), 10–23. <https://doi.org/10.3808/jei.201400266>.

1574 Niu, X.Q., Liu, C.G., Jia, X.X., Zhu, J.T., 2021. Changing soil organic carbon with land use and  
1575 management practices in a thousand-year cultivation region. *Agr. Ecosyst. Environ.* 322, 107639.  
1576 <https://doi.org/10.1016/j.agee.2021.107639>.

1577 Niu, X.Q., Jia, X.X., Yang, X.F., Wang, J., Wei, X.R., Wu, L.H., Shao, M.A., 2022. Tracing the  
1578 Sources and Fate of NO<sub>3</sub><sup>-</sup> in the Vadose Zone-Groundwater System of a Thousand-Year-  
1579 Cultivated Region. *Environ. Sci. Technol.* 56(13), 9335–9345.  
1580 <https://doi.org/10.1021/acs.est.1c06289>.

1581 Nixon, S., Trent, Z., Marcuello, C., Lallana, C., 2003. Europe’s water: An indicator-based  
1582 assessment. European Environment Agency.

1583 Ortega-Farias, S., Poblete-Echeverria, C., Brisson, N., 2010. Parameterization of a two-layer model  
1584 for estimating vineyard evapotranspiration using meteorological measurements. *Agric. For.*  
1585 *Meteorol.* 150(2), 276–286. <https://doi.org/10.1016/j.agrformet.2009.11.012>.

1586 Panchal, P., Preece, C., Peñuelas, J., Giri, J., 2022. Soil carbon sequestration by root exudates,  
1587 *Trends Plant Sci.* 27(8), 749–757. <https://doi.org/10.1016/j.tplants.2022.04.009>.

1588 Paschalis, A., Bonetti, S., Guo, Y., Fatichi, S., 2022. On the uncertainty induced by pedotransfer  
1589 functions in terrestrial biosphere modeling. *Water Resour. Res.* 58, e2021WR031871.  
1590 <https://doi.org/10.1029/2021WR031871>.

1591 Peng, X.L., Peng, L., Bai, Z.J., Liu, Y.H., 1979. Regional Evaluation of Underground Fertilizer and  
1592 Water Resources in Guanzhong Area. *Soil* 1, 21–27. (In Chinese)

1593 Power, J.F., Schepers, J.S., 1989. Nitrate contamination of groundwater in North America. *Agri*  
1594 *Ecosyst. Environ.* 26(3–4), 165–187. [https://doi.org/10.1016/0167-8809\(89\)90012-1](https://doi.org/10.1016/0167-8809(89)90012-1).

1595 Qiao, J.B., Zhu, Y.J., Jia, X.X., Huang, L.M., Shao, M.A., 2018. Estimating the spatial relationships  
1596 between soil hydraulic properties and soil physical properties in the critical zone (0–100 m) on  
1597 the Loess Plateau, China: A state-space modeling approach. *Catena* 160, 385–393.  
1598 <http://dx.doi.org/10.1016/j.catena.2017.10.006>.

1599 Rathay, S.Y., Allen, D.M., Kirste, D., 2018. Response of a fractured bedrock aquifer to recharge  
1600 from heavy rainfall events. *J Hydrol.* 561, 1048–1062.  
1601 <https://doi.org/10.1016/j.jhydrol.2017.07.042>.

1602 Rempe, D., Dietrich, W., 2018. Direct observations of rock moisture, a hidden component of the  
1603 hydrologic cycle. *Proc. Natl. Acad. Sci. USA* 115, 201800141.  
1604 <http://dx.doi.org/10.1073/pnas.1800141115>.

1605 Ren, M., Li, C.J., Gao, X.D., Niu, H.H., Cai, Y.H., Wen, H.X., Yang, M.H., Siddique, K.H.M., Zhao,  
1606 X.N., 2023. High nutrients surplus led to deep soil nitrate accumulation and acidification after  
1607 cropland conversion to apple orchards on the Loess Plateau, China. *Agr. Ecosyst. Environ.* 351,  
1608 108482. <https://doi.org/10.1016/j.agee.2023.108482>.

1609 Richardson, M., Kumar, P., 2017. Critical Zone services as environmental assessment criteria in  
1610 intensively managed landscapes, *Earths Future* 5, 617–632.  
1611 <https://doi.org/10.1002/2016EF000517>.

1612 Rosen, A.M., 2008. The impact of environmental change and human land use on alluvial valleys in  
1613 the Loess Plateau of China during the Middle Holocene. *Geomorphology* 101(1–2), 298–307.  
1614 <https://doi.org/10.1016/j.geomorph.2008.05.017>.

1615 Rumpel, C., Kögel-Knabner, I., 2011. Deep soil organic matter—a key but poorly understood  
1616 component of terrestrial C cycle. *Plant Soil* 338, 143–158. [https://doi.org/10.1007/s11104-010-](https://doi.org/10.1007/s11104-010-0391-5)  
1617 0391-5.

1618 Sadeghi, S.H., Hazbavi, Z., Kiani-Harchegani, M., Younesi, H., Sadeghi, P., Angulo-Jaramillo, R.,  
1619 Lassabatere, L., 2021. The hydrologic behavior of Loess and Marl soils in response to biochar  
1620 and polyacrylamide mulching under laboratorial rainfall simulation conditions. *J Hydrol.* 592,  
1621 125620. <https://doi.org/10.1016/j.jhydrol.2020.125620>.

1622 Salve, R., Rempe, D.M., Dietrich, W.E., 2012. Rain, rock moisture dynamics, and the rapid response  
1623 of perched groundwater in weathered, fractured argillite underlying a steep hillslope. *Water*  
1624 *Resour. Res.* 48, W11528. <https://doi.org/10.1029/2012WR012583>

1625 Schaap, M.G., Leij, F.J., Genuchten, M.T., 2001. ROSETTA: a computer program for estimating  
1626 soil hydraulic parameters with hierarchical pedotransfer functions. *J Hydrol.* 251(3–4), 163–176.  
1627 [https://doi.org/10.1016/S0022-1694\(01\)00466-8](https://doi.org/10.1016/S0022-1694(01)00466-8).

1628 Seiler, K.P., Gat, J.R., 2007. *Groundwater Recharge from Run-off, Infiltration and Percolation.*  
1629 Springer.

1630 Shao, M.A., Wang, Y.Q., Xia, Y.Q., Jia, X.X., 2018. Soil drought and water carrying capacity for  
1631 vegetation in the critical zone of the Loess Plateau: A review. *Vadose Zone J.* 17, 170077.

1632 <https://doi.org/10.2136/vzj2017.04.0077>.

1633 Shao, X.Y., Gao, X.D., Zeng, Y.J., Yang, M., Wang, Y.F., Zhao, X.N., 2023. Eco-Physiological  
1634 Constraints of Deep Soil Desiccation in Semiarid Tree Plantations. *Water Resour. Res.* 59(8),  
1635 e2022WR034246. <https://doi.org/10.1029/2022WR034246>.

1636 Shi, P., Feng, Z.H., Gao, H.D., Li, Z.B., Xu, G.C., Ren, Z.P., Xiao, L., 2020. Has “Grain for Green”  
1637 threaten food security on the Loess Plateau of China? *Ecosyst. Health Sustain.* 6, 1709560.  
1638 <https://doi.org/10.1080/20964129.2019.1709560>.

1639 Shi, P., Huang, Y.N., Ji, W.J., Xiang, W., Evaristo, J., Li, Z., 2021. Impacts of deep-rooted fruit trees  
1640 on recharge of deep soil water using stable and radioactive isotopes. *Agri. Forest Meteorol.* 300,  
1641 108325. <https://doi.org/10.1016/j.agrformet.2021.108325>.

1642 Sjögersten, S., Atkin, C., Clarke, M., Mooney, S., Wu, B., West, H.M., 2013, Responses to climate  
1643 change and farming policies by rural communities in northern China: A report on field observation  
1644 and farmers’ perception in dryland north Shaanxi and Ningxia, *Land Use Policy* 32, 125–133.  
1645 <https://doi.org/10.1016/j.landusepol.2012.09.014>.

1646 Smalley, I.J., Jefferson, I.F., Dijkstra, T.A., Derbyshire, E., 2001. Some major events in the  
1647 development of the scientific study of loess. *Earth Sci. Rev.* 54(1–3), 5–18.  
1648 [https://doi.org/10.1016/S0012-8252\(01\)00038-1](https://doi.org/10.1016/S0012-8252(01)00038-1).

1649 Song, X.L., Wu, P.T., Gao, X.D., Yao, J., Zou, Y.F., Zhao, X.N., Siddique, K.H.M., Hu, W., 2020.  
1650 Rainwater collection and infiltration (RWCI) systems promote deep soil water and organic carbon  
1651 restoration in water-limited sloping orchards. *Agric. Water Manage.* 242, 106400.  
1652 <https://doi.org/10.1016/j.agwat.2020.106400>.

1653 Souchère, V., King, C., Dubreuil, N., Lecomte-Morel, V., Bissonnais, Y.L., Chalat, M., 2003.  
1654 Grassland and crop trends: role of the European Union Common Agricultural Policy and  
1655 consequences for runoff and soil erosion. *Environmental Science and Policy* 6(1): 7–16.  
1656 [https://doi.org/10.1016/S1462-9011\(02\)00121-1](https://doi.org/10.1016/S1462-9011(02)00121-1).

1657 Spalding, R.F., Exner, M.E., Lindau, C.W., Eaton, D.W., 1982. Investigation of sources of  
1658 groundwater nitrate contamination in the Burbank-Wallula area of Washington, USA. *J. Hydrol.*  
1659 58(3–4), 307–324. [https://doi.org/10.1016/0022-1694\(82\)90041-5](https://doi.org/10.1016/0022-1694(82)90041-5)

1660 Sun, Y.B., Clemens, S.C., Guo, F., Liu, X.X., Wang, Y., Yan, Y., Liang, L.J., 2021. High-  
1661 sedimentation-rate loess records: A new window into understanding orbital- and millennial-scale  
1662 monsoon variability. *Earth-Sci. Rev.* 220, 103731.  
1663 <https://doi.org/10.1016/j.earscirev.2021.103731>.

1664 Tan, H.B., Wen, X.W., Rao, W.B., Bradd, J., Huang, J.Z., 2016. Temporal variation of stable isotopes  
1665 in a precipitation–groundwater system: implications for determining the mechanism of  
1666 groundwater recharge in high mountain–hills of the Loess Plateau, China. *Hydrol. Process.* 30,  
1667 1491–1505. <https://doi.org/10.1002/hyp.10729>.

1668 Triplett, G.B., Dabney, S.M., Siefker, J.H., 1996. Tillage systems for cotton on silty upland soils.  
1669 *Agronomy J.* 88(4), 507–512. <https://doi.org/10.2134/agronj1996.00021962008800040002x>.

1670 Turkeltaub, T., Jia, X.X., Zhu, Y.J., Shao, M.A., Binley, A., 2018. Recharge and nitrate transport  
1671 through the deep vadose zone of the Loess Plateau: a regional-scale model investigation. *Water*  
1672 *Resour. Res.* 54, 4332–4346. <https://doi.org/10.1029/2017WR022190>.

1673 Turkeltaub, T., Wang, J., Cheng, Q.B., Jia, X.X., Zhu, Y.J., Shao, M.A., Binley, A., 2022. Soil  
1674 moisture and electrical conductivity relationships under typical Loess Plateau land covers. *Vadose*  
1675 *Zone J.* 21, e20174. <https://doi.org/10.1002/vzj2.20174>.

1676 Turkeltaub, T., Bel, G., 2023. The effects of rain and evapotranspiration statistics on groundwater  
1677 recharge estimations for semi-arid environments. *Hydrol. Earth Syst. Sci.* 27(1), 289–302.  
1678 <https://doi.org/10.5194/hess-27-289-2023>.

1679 Vereecken, H., Huisman, J.A., Hendricks Franssen, H.J., Brüggemann, N., Bogaen, H.R., Kollet, S.,  
1680 Javaux, M., Kruk, J.V.J., Vanderborght, J., 2015. Soil hydrology: Recent methodological  
1681 advances, challenges, and perspectives. *Water Resour. Res.* 51(4), 2616–2633.  
1682 <https://doi.org/10.1002/2014WR016852>.

1683 Vereecken, H., Amelung, W., Bauke, S., Bogaen, H., Brüggemann, N., Montzka, C., Vanderborght,  
1684 J., Bechtold, M., Blöschl, G., Carminati, A., Javaux, M., Konings, A., Kusche, J., Neuweiler, I.,  
1685 Or, D., Steele-Dunne, S., Verhoef, A., Young, M., Zhang, Y., 2022. Soil hydrology in the Earth  
1686 system. *Nat. Rev. Earth Environ.* 3, 573–587. <https://doi.org/10.1038/s43017-022-00324-6>.

1687 Walvoord, M.A., Phillips, F.M., Stonestrom, D.A., Striegl, R.G., et al., 2003. A Reservoir of Nitrate  
1688 Beneath Desert Soils. *Science*, 302, 1021–1024. <https://doi.org/10.1126/science.1086435>

1689 Wang, D.Q., 1982. The characteristics of groundwater recharge on the Luochuan tableland.  
1690 *Hydrogeol. Eng. Geol.* 9(5), 1–8 (In Chinese).

1691 Wang, Y., Shao, M.A., Shao, H.B., 2010. A preliminary investigation of the dynamic characteristics  
1692 of dried soil layers on the Loess Plateau of China. *J Hydrol.* 381(1–2), 9–17.  
1693 <https://doi.org/10.1016/j.jhydrol.2009.09.042>.

1694 Wang, Y., Shao, M.A., Zhu, Y.J., Liu, Z.P., 2011. Impacts of land use and plant characteristics on  
1695 dried soil layers in different climatic regions on the Loess Plateau of China. *Agric. For. Meteorol.*  
1696 151(4), 437–448. <https://doi.org/10.1016/j.agrformet.2010.11.016>.

1697 Wang, Q.X., Fan, X.H., Qin, Z.D., Wang, M.B., 2012. Change trends of temperature and  
1698 precipitation in the Loess Plateau Region of China, 1961–2010, *Global Planet. Change* 92–93,  
1699 138–147. <https://doi.org/10.1016/j.gloplacha.2012.05.010>.

1700 Wang, Y.Q., Shao, M.A., Liu, Z.P., Zhang, C.C., 2015a. Characteristics of dried soil layers under  
1701 apple orchards of different ages and their applications in soil water managements on the Loess  
1702 Plateau of China. *Pedosphere* 25(4), 546–554. [https://doi.org/10.1016/S1002-0160\(15\)30035-7](https://doi.org/10.1016/S1002-0160(15)30035-7).

1703 Wang, Y.Q., Shao, M.A., Zhang, C.C., Liu, Z.P., Zou, J.L., Xiao, J.F., 2015b. Soil organic carbon in  
1704 deep profiles under Chinese continental monsoon climate and its relations with land uses. *Ecol.*  
1705 *Eng.* 82, 361–367. <https://doi.org/10.1016/j.ecoleng.2015.05.004>

1706 Wang, S., Fu, B.J., Piao, S.L., Lü, Y.H., Ciais, P., Feng, X.M., Wang, Y.F., 2016a. Reduced sediment  
1707 transport in the Yellow River due to anthropogenic changes. *Nat. Geosci.* 9, 38–41.  
1708 <http://dx.doi.org/10.1038/NGEO2602>.

1709 Wang, Y.Q., Han, X.W., Jin, Z., Zhang, C.C., Fang, L.C., 2016b. Soil organic carbon stocks in deep  
1710 soils at a watershed scale on the Chinese loess plateau. *Soil Sci. Soc. Am. J.* 80, 157–167.  
1711 <https://doi.org/10.2136/sssaj2015.06.0220>.

1712 Wang, Y.Q., Hu, W., Sun, H., Zhao, Y.L., Zhang, P.P., Li, Z.M., Zhou, Z.X., Tong, Y.P., Liu, S.Z.,  
1713 Zhou, J.X., Huang, M.B., Jia, X.X., Clothier, B., Shao, M.A., Zhou, W.J., An, Z.S., 2024. Soil  
1714 moisture decline in China’s monsoon loess critical zone: More a result of land-use conversion  
1715 than climate change. *P. Natl. Acad. Sci. USA* 121(15), e2322127121.  
1716 <https://doi.org/10.1073/pnas.2322127121>.

1717 Wang, Q.M., Fan, J., Wang, S., Yong, C.X., Ge, J.M., You, W., 2019a. Application and accuracy of  
1718 cosmic-ray neutron probes in three soil textures on the Loess Plateau, China. *J. Hydrol.* 569, 449–  
1719 461. <https://doi.org/10.1016/j.jhydrol.2018.11.073>.

1720 Wang, S., Fan, J., Ge, J.M., Wang, Q.M., Fu, W., 2019b. Discrepancy in tree transpiration of *Salix*  
1721 *matsudana*, *Populus simonii* under distinct soil, topography conditions in an ecological  
1722 rehabilitation area on the Northern Loess Plateau. *Forest Ecol. Manag.* 432, 675–685.  
1723 <https://doi.org/10.1016/j.foreco.2018.10.011>.

1724 Wang, K., Zhang, X.Y., Ma, J.B., Ma, Z.H., Li, G.L., Zheng, J.Y., 2020. Combining infiltration holes  
1725 and level ditches to enhance the soil water and nutrient pools for semi-arid slope shrubland  
1726 revegetation. *Sci Total Environ.* 729, 138796. <https://doi.org/10.1016/j.scitotenv.2020.138796>.

1727 Wang, K.B., Deng, L., Shangguan, Z.P., Chen, Y.P., Lin, X., 2021a. Sustainability of eco-  
1728 environment in semi-arid regions: Lessons from the Chinese Loess Plateau, *Environ. Sci. Policy*  
1729 125, 126–134. <https://doi.org/10.1016/j.envsci.2021.08.025>.

1730 Wang, K., Zhang, X.Y., Li, G.L., Ma, J.B., Zhang, S.Q., Zheng, J.Y., 2021b. Effect of using an  
1731 infiltration hole and mulching in fish-scale pits on soil water, nitrogen, and organic matter  
1732 contents: Evidence from a 4-year field experiment. *Land Degrad Dev.* 32, 4203–4211.  
1733 <https://doi.org/10.1002/ldr.4026>.

1734 Wang, G.H., Chen, Z.X., Shen, Y.Y., Yang, X.L., 2023a. Thinning promoted the rejuvenation and  
1735 highly efficient use of soil water for degraded *Caragana korshinskii* plantation in semiarid loessal  
1736 regions. *Land Degrad Dev.* 34(4), 992–1003. <https://doi.org/10.1002/ldr.4511>.

1737 Wang, S.F., Yang, M., Gao, X.D., Hu, Q., Song, J.J., Ma, N.F., Song, X.L., Siddique, K.H.M., Wu,  
1738 P.T., Zhao, X.N., 2023b. Divergent responses of deep SOC sequestration to large-scale  
1739 revegetation on China's Loess Plateau. *Agri. Ecosyst. Environ.* 349, 108433.  
1740 <https://doi.org/10.1016/j.agee.2023.108433>.

1741 Wei, W., Chen, D., Wang, L.X., Daryanto, S., Chen, L.D., Yu, Y., Lu, Y.L., Sun, G., Feng, T.J., 2016a.  
1742 Global synthesis of the classification, distributions, benefits and issues of terracing. *Earth Sci.*  
1743 *Rev.* 159, 388–403. <https://doi.org/10.1016/j.earscirev.2016.06.010>.

1744 Wei, X.R., Zhang, Y.J., Liu, J., Gao, H.L., Fan, J., Jia, X.X., Cheng, J.M., Shao, M.A., Zhang, X.C.,  
1745 2016b. Response of soil CO<sub>2</sub> efflux to precipitation manipulation in a semiarid grassland. *J*  
1746 *Environ. Sci.* 45, 207–214. <https://doi.org/10.1016/j.jes.2016.01.008>.

1747 Wei, W., Pan, D.L., Yang, Y., 2021. Effects of terracing measures on water retention of *Pinus*  
1748 *Tabulaeformis* forest in the dryland loess hilly region of China. *Agr. Forest Meteorol.* 308–309,  
1749 108544. <https://doi.org/10.1016/j.agrformet.2021.108544>.

1750 Wen, X., Zhen, L., 2020. Soil erosion control practices in the Chinese Loess Plateau: a systematic  
1751 review. *Environ. Dev.* 34, 100493. <https://doi.org/10.1016/j.envdev.2019.100493>.

1752 Whittle, A.W.R., Whittle, A.W.R., 1996. *Europe in the Neolithic: The creation of new worlds*,  
1753 Cambridge world archaeology. Cambridge University Press, New York.

1754 Wilson, C.G., and other 34 authors, 2018. The Intensively Managed Landscape Critical Zone  
1755 Observatory: A Scientific Testbed for Understanding Critical Zone Processes in Agroecosystems.  
1756 *Vadose Zone J.* 17, 180088. <https://doi.org/10.2136/vzj2018.04.0088>.

1757 World Health Organization, 2007. *Nitrate and Nitrite in Drinking Water*. World Health Organization,  
1758 Geneva, Switzerland.

1759 Worrall, F., Howden, N.J.K., Burt, T.P., 2015. Evidence for nitrogen accumulation: the total nitrogen  
1760 budget of the terrestrial biosphere of a lowland agricultural catchment. *Biogeochemistry* 123,  
1761 411–428. <https://doi.org/10.1007/s10533-015-0074-7>

1762 Xia, Y.Q., Shao, M.A., 2008. Soil water carrying capacity for vegetation: A hydrologic and  
1763 biogeochemical process model solution. *Ecol. Model.* 214, 112–124.

1764 <https://doi.org/10.1016/j.ecolmodel.2008.01.024>.

1765 Xia, Y.Q., Shao, M.A., 2009. Evaluation of soil water-carrying capacity for vegetation: The concept  
1766 and the model. *Acta Agric. Scand.* 59, 342–348. <https://doi.org/10.1080/09064710802203537>.

1767 Xiang, W., Si, B.C., Biswas, A., Li, Z., 2019. Quantifying dual recharge mechanisms in deep  
1768 unsaturated zone of Chinese Loess Plateau using stable isotopes. *Geoderma* 337, 773–781.  
1769 <https://doi.org/10.1016/j.geoderma.2018.10.006>.

1770 Xiang, W., Evaristo, J., Li, Z., 2020. Recharge mechanisms of deep soil water revealed by water  
1771 isotopes in deep loess deposits. *Geoderma* 369, 114321.  
1772 <https://doi.org/10.1016/j.geoderma.2020.114321>.

1773 Xu, J., 2001. Historical bank-breachings of the lower Yellow River as influenced by drainage basin  
1774 factors. *Catena* 45, 1–17. [https://doi.org/10.1016/S0341-8162\(01\)00136-9](https://doi.org/10.1016/S0341-8162(01)00136-9).

1775 Xu, X., Chen, T., 2010. Experimental study on infiltration of loess column through preferential flow.  
1776 *J. Soil Water Conserv.* 24(4), 82–85 (In Chinese).  
1777 <https://doi.org/10.13870/j.cnki.stbcb.2010.04.023>

1778 Yan, T.B., 1986. Discussion on the renewal period of groundwater on the Loess Tableland.  
1779 *Hydrogeol. Eng. Geol.* 1(3), 42–44 (In Chinese). <https://doi.org/10.16030/j.cnki.issn.1000-3665.1986.03.012>

1781 Yang, X.P., Liu, T., Yuan, B.Y., 2009. The Loess Plateau of China: Aeolian sedimentation and fluvial  
1782 erosion, both with superlative rates. *Geomorphol. Land. World* 1, 275–282.  
1783 <https://doi.org/10.1007/978-90-481-3055-9-28>

1784 Yang, K.Q., Liu, H.T., Ning, J.Y., Zhen, Q., Zheng, J.Y., 2023. Rainwater infiltration and nutrient  
1785 recharge system significantly enhance the growth of degraded artificial forest in semi-arid areas  
1786 with shallowly buried soft bedrock. *Forest Ecol. Manag.* 539, 121016.  
1787 <https://doi.org/10.1016/j.foreco.2023.121016>.

1788 Yang, M., Gao, X., Wang, S., Zhao, X., 2022. Quantifying the importance of deep root water uptake  
1789 for apple trees' hydrological and physiological performance in drylands. *J Hydrol.* 606(11),  
1790 127471. <https://doi.org/10.1016/j.jhydrol.2022.127471>.

1791 Yao, Y., Song, J., Wei, X., 2022. The fate of carbon in check dam sediments. *Earth–Sci. Rev.* 224,  
1792 103889. <https://doi.org/10.1016/j.earscirev.2021.103889>.

1793 Zech, R.A., 2012. A permafrost glacial hypothesis-Permafrost carbon might help explaining the  
1794 Pleistocene ice ages. *Quat. Sci. J.* 61, 84–92. <https://doi.org/10.3285/eg.61.1.07,2012>.

1795 Zeng, Y., Ran, L.S., Fang, N.F., Wang, Z., Xu, Z.C., Lu, X.X., Yu, Q., Wang, L., Yu, S.X., Shi, Z.H.,  
1796 2022. How to balance green and grain in marginal mountainous areas? *Earths Future* 10,  
1797 e2021EF002552. <https://doi.org/10.1029/2021EF002552>.

1798 Zhang, X., An, Z., 1994. Relationship between forests and loess thicknesses in the Loess Plateau  
1799 region. *Bull. Soil Water Conserv.* 14, 1–4. (In Chinese)  
1800 <https://doi.org/10.13961/j.cnki.stbctb.1994.06.001>.

1801 Zhang, X., An, Z., Chen, Y., 1998. Revegetation and lithological composition in semiarid regions.  
1802 *Acta Geogr. Sin.* 53, 134–140. (In Chinese).

1803 Zhang, Y., Huang, M.B., Lian, J.J., 2015. Spatial distributions of optimal plant coverage for the  
1804 dominant tree and shrub species along a precipitation gradient on the central Loess Plateau. *Agri.  
1805 Forest Meteo.* 206, 69–84. <http://dx.doi.org/10.1016/j.agrformet.2015.03.001>.

1806 Zhang, S.L., Yang, D.W., Yang, Y.T., Piao, S.L., Yang, H.B., Lei, H.M., Fu, B.J., 2018a. Excessive  
1807 afforestation and soil drying on China's Loess Plateau. *J. Geophys. Res.: Biogeosci.* 123, 923–

1808 935. <https://doi.org/10.1002/2017JG004038>.

1809 Zhang, Z.Q., Li, M., Si, B.C., Feng, H., 2018b. Deep rooted apple tress decrease groundwater  
1810 recharge in the highland region of the Loess Plateau, China. *Sci. Total Environ.* 622–623, 584–  
1811 593. <https://doi.org/10.1016/j.scitotenv.2017.11.230>.

1812 Zhang, G.L., Zhu, Y.G., Shao, M.A., 2019. Understanding sustainability of soil and water resources  
1813 in a critical zone perspective. *Sci. China Earth Sci.* 62, 1716–1718.  
1814 <https://doi.org/10.1007/s11430-019-9368-7>.

1815 Zhang, X.Y., Wang, K., Li, G.L., Zheng, J.Y., 2023. Infiltration holes enhance the deep soil water  
1816 replenishment in level ditch on the Loess Plateau of China. *Land Degrad. Dev.* 34(5),1549–1557.  
1817 <https://doi.org/10.1002/ldr.4552>.

1818 Zhang, Z.D., Jia, X.X., Zhu, P., Huang, M.B., Ren, L.D., Shao, M.A., 2024. Estimating the optimal  
1819 vegetation coverage for the dominant tree and shrub species over China’s northwest drylands. *Sci.*  
1820 *China Earth Sci.* 67, <https://doi.org/10.1007/s11430-023-1287-x>.

1821 Zhao, Y., Wang, L., 2021. Determination of groundwater recharge processes and evaluation of the  
1822 ‘two water worlds’ hypothesis at a check dam on the Loess Plateau. *J Hydrol.* 595, 125989.  
1823 <https://doi.org/10.1016/j.jhydrol.2021.125989>.

1824 Zhao, G., Mu, X., Wen, Z., Wang, F., Gao, P., 2013. Soil erosion, conservation, and eco-environment  
1825 changes in the Loess Plateau of China. *Land Degrad. Dev.* 24, 499–510.  
1826 <https://doi.org/10.1002/ldr.2246>.

1827 Zhao, C.L., Shao, M.A., Jia, X.X., Zhu, Y.J., 2019. Factors affecting soil desiccation spatial  
1828 variability in the Loess Plateau of China. *Soil Sci. Soc. Am. J.* 83, 266–275.  
1829 <https://doi.org/10.2136/sssaj2017.11.0391>.

1830 Zhao, C.L., Jia, X.X., Shao, M.A., Zhang, X.B., 2020. Using pedo-transfer functions to estimate dry  
1831 soil layers along an 860-km long transect on China’s Loess Plateau. *Geoderma* 369, 114320.  
1832 <https://doi.org/10.1016/j.geoderma.2020.114320>.

1833 Zhao, C.L., Shao, M.A., Jia, X.X., Zhu, Y.J., 2021. Regional variations in plant-available soil water  
1834 storage and related driving factors in the middle reaches of the Yellow River Basin, China. *Agric.*  
1835 *Water Manage.* 257, 107131. <https://doi.org/10.1029/j.agwat.2021.107131>.

1836 Zheng, X., Yao, S.B., Lu, Y.N., 2020. Impacts of sloping land conversion program on Grain  
1837 Production-A case study in Shanxi Province, *Bull. Soil Water Cons.* 40(2), 239–246 (In Chinese).  
1838 <http://doi.org/10.13961/j.cnki.stbctb.2020.02.035>.

1839 Zhu, X.M., 1964. *Lou Soils*. Agriculture Press, Beijing (In Chinese).

1840 Zhu, Y.G., Li, G., Zhang, G.L., Fu, B.J., 2015a. Soil security: From Earth’s critical zone to  
1841 ecosystem services. *Acta Geogr. Sin.* 70(12), 1859–1869. (In Chinese)  
1842 <https://doi.org/10.11821/dlxb201512001>.

1843 Zhu, H.X., Fu, B.J., Wang, S., Zhu, L.H., Zhang, L.W., Jiao, L., Wang, C., 2015. Reducing soil  
1844 erosion by improving community functional diversity in semi-arid grasslands. *J. Applied Ecology*,  
1845 52, 1063–1072. <https://doi.org/10.1111/1365-2664.12442>.

1846 Zhu, Y.J., Jia, X.X., Shao, M.A., 2018. Loess thickness variations across the Loess Plateau of China.  
1847 *Surv. Geophys.* 39, 715–727. <https://doi.org/10.1007/s10712-018-9462-6>.

1848 Zhu, Y.J., Jia, X.X., Qiao, J.B., Binley, A., Horton, R., Hu, W., Wang, Y.Q., Shao, M.A., 2019.  
1849 Capacity and distribution of water stored in the vadose zone of the Chinese Loess Plateau. *Vadose*  
1850 *Zone J.* 18, 180203. <https://doi.org/10.2136/vzj2018.11.0203>.

1851 Zhu, X.Q., Fu, W.H., Kong, X.G., Chen, C.X., Liu, Z.J., Chen, Z.J., Zhou, J.B., 2021. Nitrate

1852 accumulation in the soil profile is the main fate of surplus nitrogen after land-use change from  
1853 cereal cultivation to apple orchards on the Loess Plateau. *Agr. Ecosyst. Environ.* 319, 107574.  
1854 <https://doi.org/10.1016/j.agee.2021.107574>.  
1855



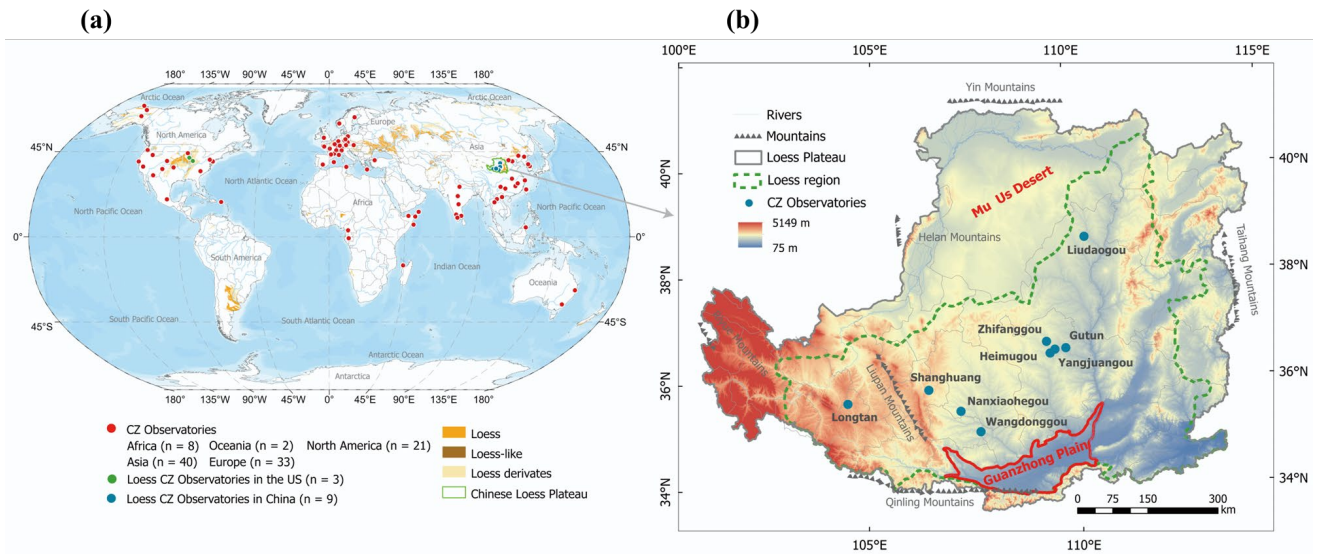


**Fig. 1** Worldwide distribution of loess deposits and Critical Zone Observatories (CZO) (a) and the representative watershed CZOs on the Chinese Loess Plateau (CLP) (b). In the CLP, there are nine monitoring sites, constituting the CLP CZO's network. These monitoring sites focus on critical soil, water, and vegetation processes in both land surface and deeper subsurface layers (down to groundwater or weathered bedrock).

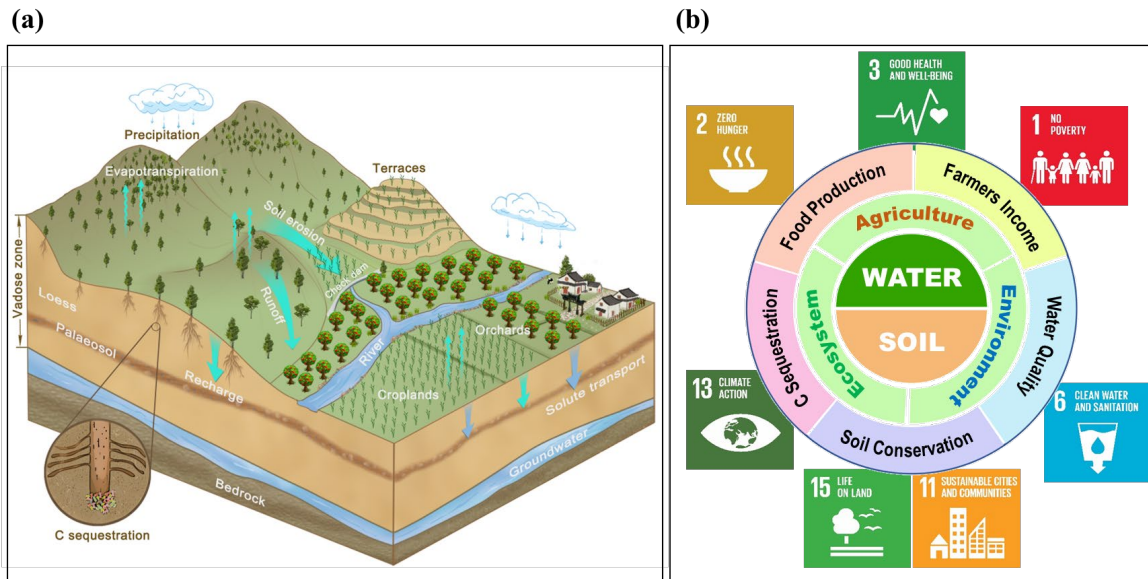


**Fig. 2** Critical soil and water processes in the Loess Critical Zone (a) and the relationship of the soil and water processes, the CZ services and seven UN Sustainable Development Goals (b) [SDG 1, No poverty; SDG 2, Zero hunger; SDG 3, Good health and well-being; SDG 6, Clean water and sanitation; SDG 11, Sustainable cities and communities; SDG 13, Climate action; SDG 15, Life on land].

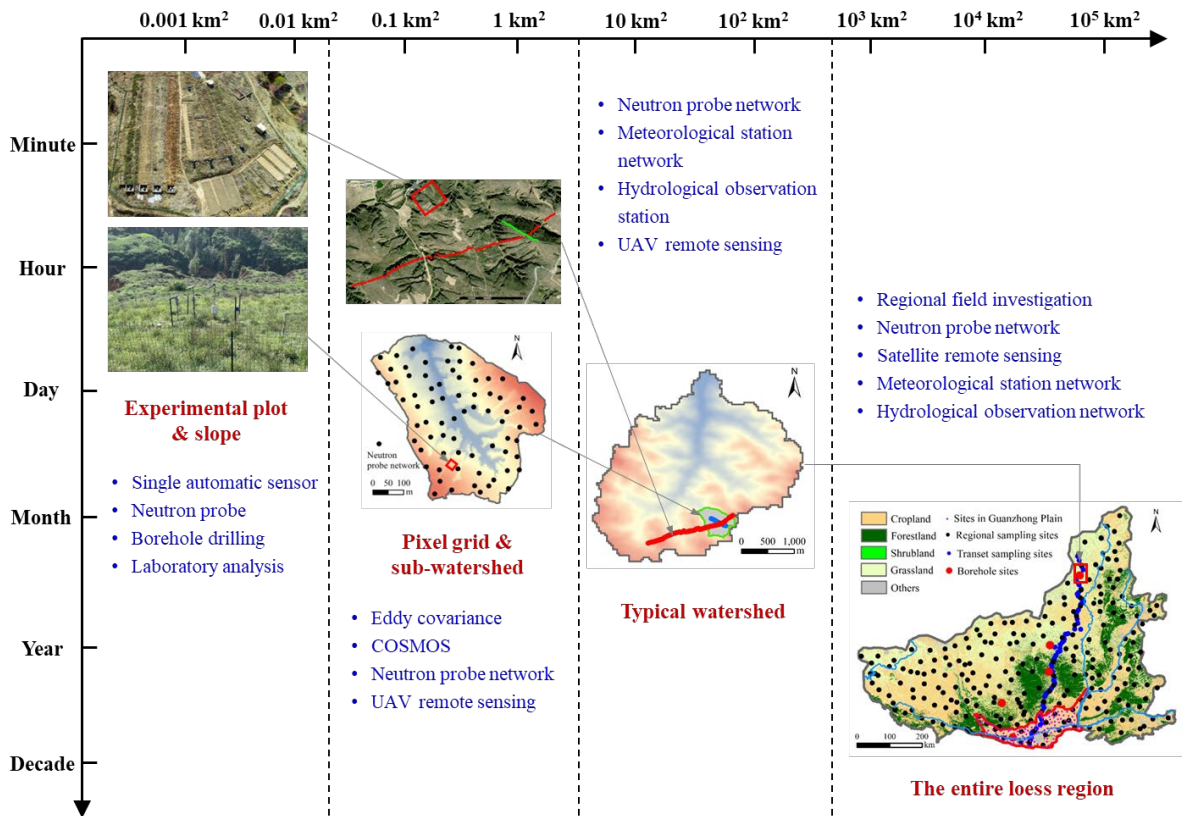


**Fig. 3** Schematic diagram of the multiscale observation system on the CLP. UAV: unmanned aerial vehicle; COSMOS: cosmic-ray soil moisture observation system.

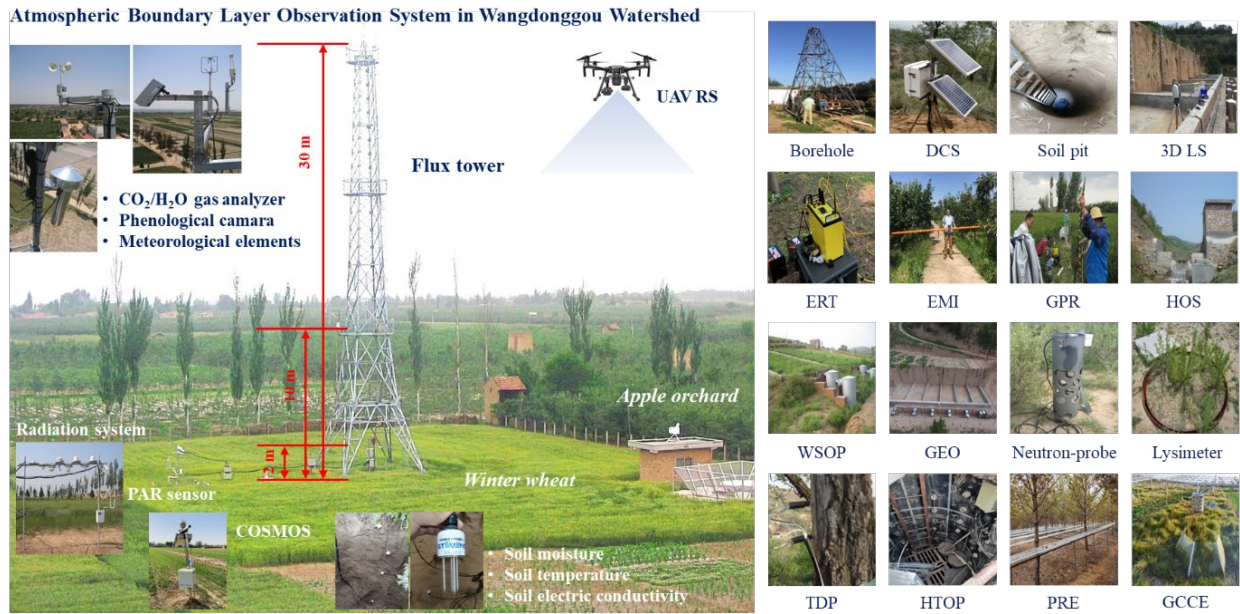


**Fig. 4** Instrumentation configuration of the grid- and plot-scale observation system at the Wangdonggou Watershed Critical Zone Observatory. UAV RS: unmanned aerial vehicle remote sensing; COSMOS: cosmic-ray soil moisture observation system; DCS: data collection system; 3D LS: 3-D laser scanner; ERT: electrical resistivity tomography; EMI: electromagnetic induction; GPR: ground penetrating radar; HOS: hydrological observation station; WSOP: water balance and sediment observation plot; GEO: gravitational erosion observation system; TDP: thermal dissipation probes; HTOP: hydrothermal observation profile; PRE: precipitation reduction experiment; GCCE: global climate change experiment.

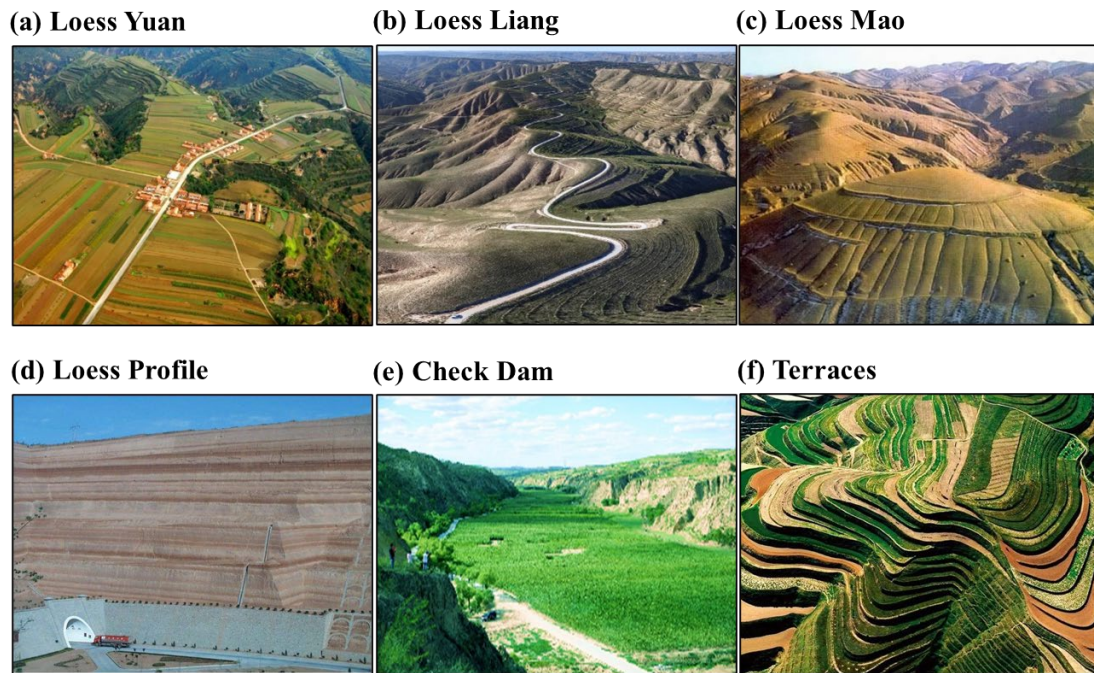


**Fig. 5** Typical loess landforms are (a) Loess Yuan, (b) Loess Liang, and (c) Loess Mao. (d) A loess profile, (e) check dams and (f) terraces on the Chinese Loess Plateau. Figure modified from the Institute of Soil and Water Conservation, CAS.

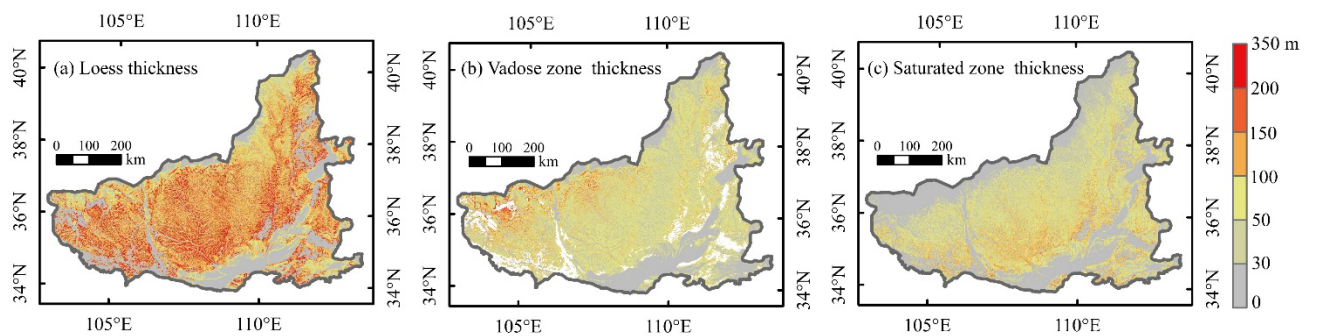


**Fig. 6** Maps of loess thickness (a), vadose zone thickness (b), and saturated zone thickness (c) across the CLP. Figures are adapted from [Zhu et al., \(2018\)](#).

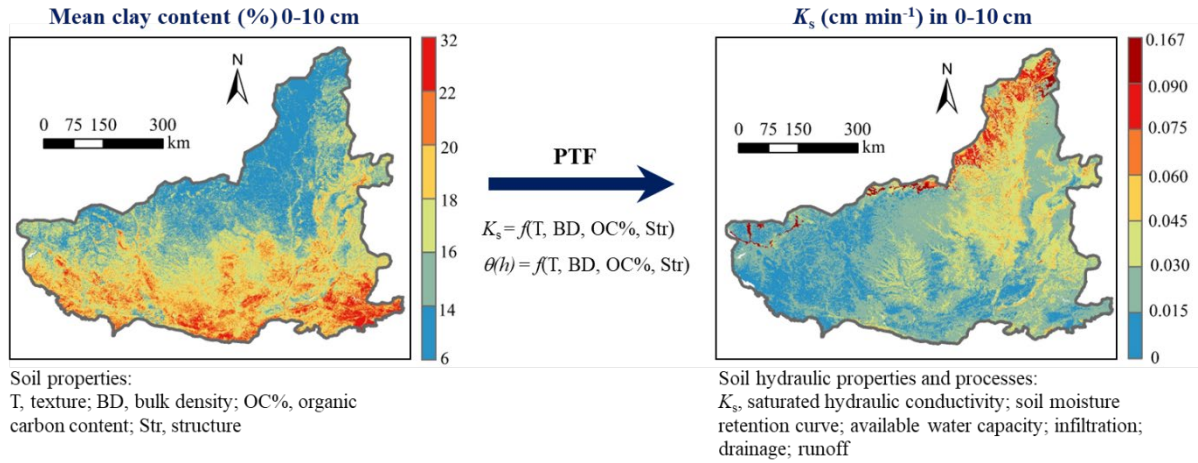


**Fig. 7** Pedotransfer functions (PTF) were developed to estimate soil hydraulic property values from selected soil property values. Estimated hydraulic property values can then serve as a basis to estimate large-scale soil hydrological processes, such as available water capacity, infiltration, drainage, and runoff. Figures are adapted from [Bai et al., \(2022\)](#).

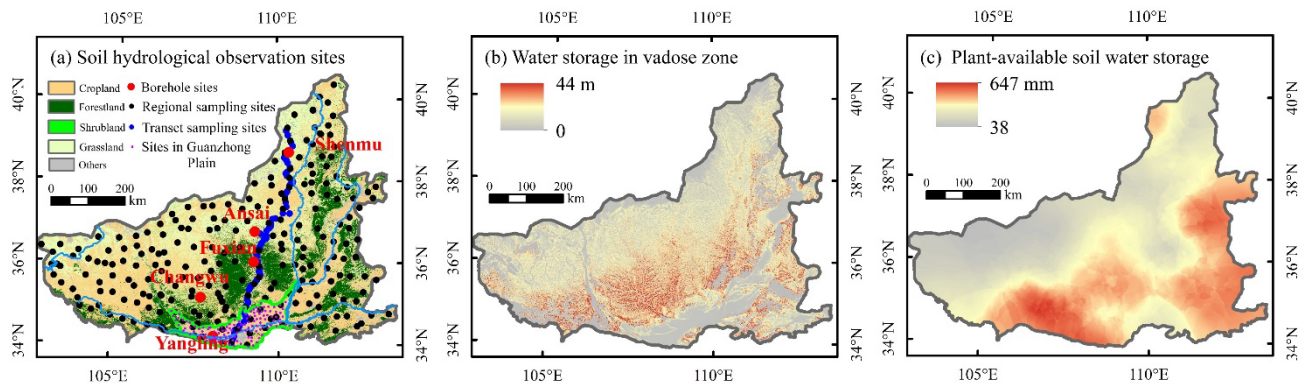


**Fig. 8** Maps of soil hydrological observation sites (a), water storage in vadose zone (b), and plant-available soil water storage (PASWS) in the 0-5 m soil layer (c) across the CLP. The PASWS was calculated as the difference between the measured SWS ( $SWS_m$ ) and the SWS at the wilting point ( $SWS_{wp}$ ). The PASWS was equal to zero when  $SWS_m$  was less than  $SWS_{wp}$ . Figures are adapted from [Cao et al., \(2018\)](#), [Zhu et al., \(2019\)](#) and [Zhao et al., \(2021\)](#).

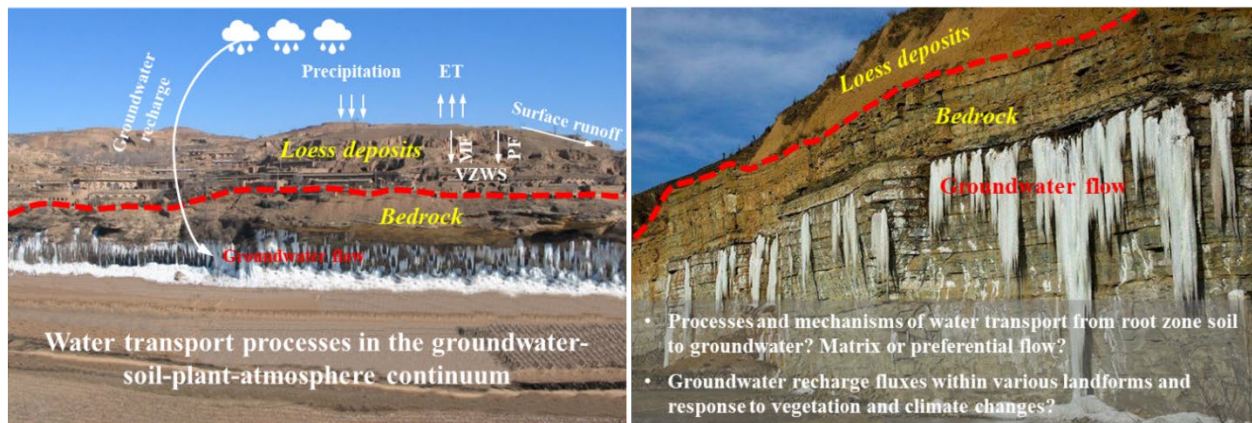


**Fig. 9** A schematic diagram of hydrological processes in the Loess Critical Zone, including evapotranspiration (ET), surface runoff, vadose zone water storage (VZWS), groundwater recharge, and water seepage through weathered bedrock. Typically, water flows either through the matrix flow (MF) or through preferential flow (PF) paths.

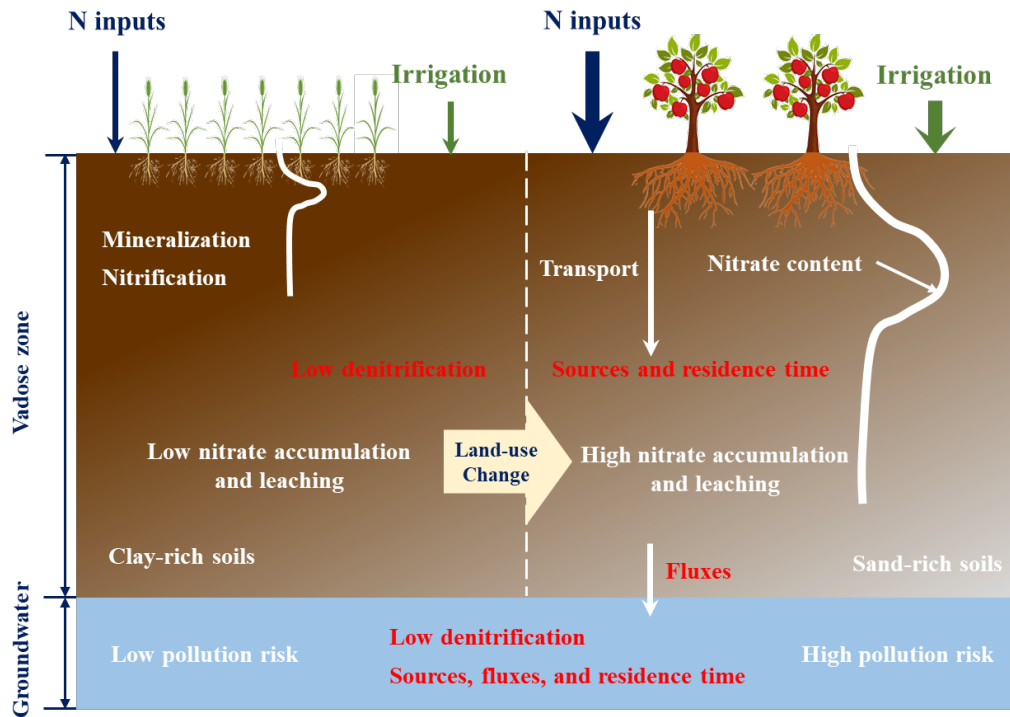


**Fig. 10** Sketch illustrating the effect of agricultural land-use change from cropland to orchard on nitrate accumulation and transport in the vadose zone-groundwater system.



# **Bringing Ancient Loess Critical Zones into A New Era of Sustainable Development Goals**

Xiaoxu Jia<sup>1,2,3</sup>, Ping Zhu<sup>1,2</sup>, Xiaorong Wei<sup>3\*</sup>, Yuanjun Zhu<sup>3</sup>, Mingbin Huang<sup>3</sup>, Wei Hu<sup>4</sup>, Yunqiang Wang<sup>5</sup>, Tuvia Turkeltaub<sup>6</sup>, Andrew Binley<sup>7</sup>, Robert Horton<sup>8</sup>, Ming'an Shao<sup>1,2,3\*</sup>

<sup>1</sup>Key Laboratory of Ecosystems Network Observation and Modeling, Institute of Geographic Sciences and Natural Resources Research, Chinese Academy of Sciences, Beijing 100101, China

<sup>2</sup>College of Resources and Environment, University of Chinese Academy of Sciences, Beijing 100190, China

<sup>3</sup>State Key Laboratory of Soil Erosion and Dryland Farming on the Loess Plateau, Northwest A&F University, Yangling, Shaanxi 712100, China

<sup>4</sup>New Zealand Inst Plant & Food Res Ltd, Private Bag 4704, Christchurch 8140, New Zealand

<sup>5</sup>State Key Laboratory of Loess and Quaternary Geology, Institute of Earth Environment, Chinese Academy of Sciences, Xi'an, Shaanxi 710061, China

<sup>6</sup>Zuckerberg Institute for Water Research, Blaustein Institutes for Desert Research, Ben-Gurion University of the Negev, Sede Boqer Campus 8499000, Israel

<sup>7</sup>Lancaster Environment Centre, Lancaster University, Bailrigg, Lancaster, LA1 4YQ, UK

<sup>8</sup>Iowa State University, Ames, Iowa 50011, USA

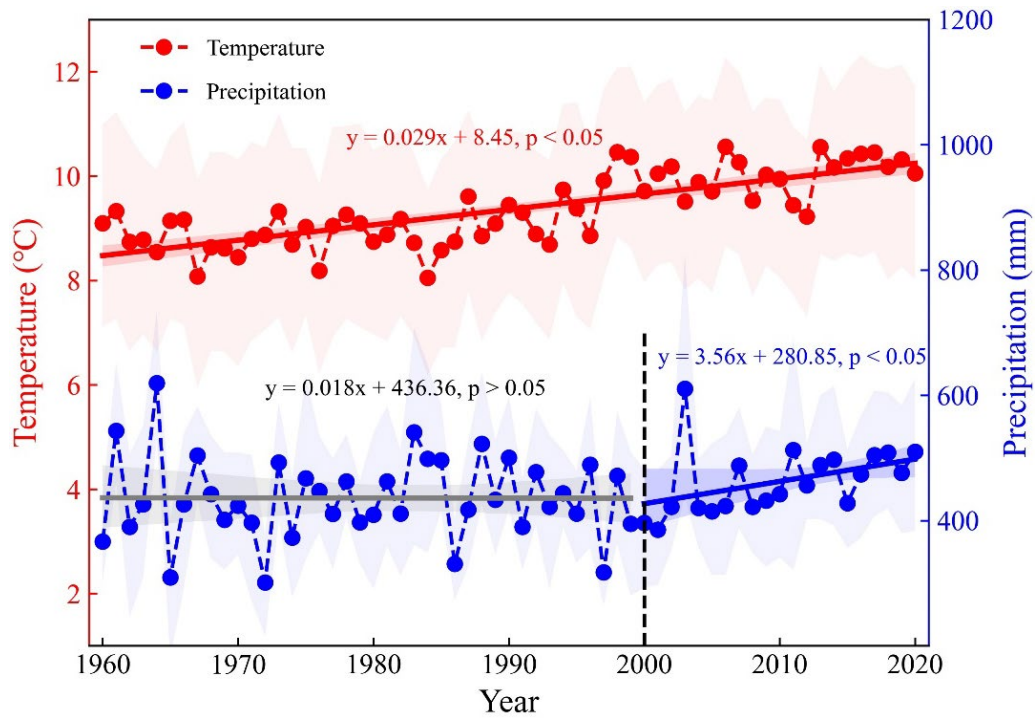


**Figure S1.** Interannual variation and monotonic trends in the annual temperature (*red*) and the amount of precipitation (*blue*) on China's Loess Plateau during 1960-2020. The lines denote the linear fits.

**Table S1** Basic information for the representative Loess CZ Observatories on China's Loess Plateau.

Watershed	Longitude	Latitude	Area (km <sup>2</sup> )	MAP (mm)	MAT (°C)	Elevation (m)	Water table (m)	Land use	Soil type	Landform
Wangdonggou	107.67	35.20	8	592	9.5	1100-1300	80	Cropland (winter wheat and maize), apple orchards, grassland (e.g., <i>S. bungeana</i> ), shrubland (e.g., <i>C. korshinskii</i> ), and forestland (e.g., <i>R. pseudoacacia</i> )	Heilutu silt loam	Tableland-gully region
Zhifanggou	109.32	36.86	8	512	9.2	1010-1430	66	Cropland (millet and maize), grassland (e.g., <i>A. gmelinii</i> , <i>A. giraldii</i> , <i>L. davurica</i> , and <i>S. bungeana</i> ), shrubland (e.g., <i>C. korshinskii</i> , <i>H. rhamnoides</i> , and <i>S. viciifolia</i> ), and forestland (e.g., <i>R. pseudoacacia</i> )	Loessial soil	Hilly-gully region
Liudaogou	110.37	38.80	7	425	9.1	1080-1270	35	Cropland (millet and maize), grassland (e.g., <i>S. bungeana</i> and <i>M. sativa</i> ), shrubland (e.g., <i>C. korshinskii</i> , <i>S. psammophila</i> , and <i>A. desertorum</i> ), orchard (e.g., <i>A. vulgaris</i> ) and forestland (e.g., <i>P. Simonii</i> and <i>P. tabuliformis</i> )	Loessial Mein soil and aeolian sand soil	Hilly-gully region
Shanghuang	106.43	36.00	8	422	7.0	1500-2000	56	Cropland (millet and maize), grassland (e.g., <i>S. grandis</i> and <i>M. sativa</i> ), shrubland (e.g., <i>C. korshinskii</i> ) and orchard (e.g., <i>P. armeniaca</i> )	Heilutu silt loam and Loessial Mein soil	Hilly region
Heimugou	109.40	36.64	8	600	10.0	1000-1200	65	Cropland (millet and maize), grassland (e.g., <i>S. bungeana</i> and <i>B. ischaemum</i> ), shrubland (e.g., <i>S. viciifolia</i> , <i>E. pungens</i> , and <i>R. xanthina</i> ), orchard (e.g., <i>P. persica</i> ) and forestland (e.g., <i>P. orientalis</i> , <i>R. pseudoacacia</i> and <i>P. tabuliformis</i> )	Heilutu silt loam	Tableland region
Gutun	109.79	36.72	42	500	9.1	900-1280	63	Cropland (millet and <i>S. italica</i> ), grassland (e.g., <i>S. bungeana</i> ), shrubland (e.g., <i>H. rhamnoides</i> , and <i>A. fruticosa</i> ), orchard (e.g., <i>M. pumila</i> ) and forestland (e.g., <i>R. pseudoacacia</i> )	Heilutu silt loam and Loessial Mein soil	Hilly-gully region
Longtan	104.48	35.74	16	386	6.8	1850-2200	66	Cropland (millet and maize), grassland (e.g., <i>S. bungeana</i> , <i>L. secalinus</i> , <i>S. grandis</i> and <i>M. sativa</i> ), shrubland (e.g., <i>C. korshinskii</i> ), apple orchards and forestland (e.g., <i>P. tabuliformis</i> )	Loessial Mein soil	Hilly-gully region
Nanxiaohogou	107.20	35.59	27	523	9.3	1050-1420	71	Cropland (millet and <i>S. italica</i> ), grassland (e.g., <i>M. sativa</i> ), shrubland (e.g., <i>S. davidii</i> and <i>H. rhamnoides</i> ), orchard (e.g., <i>P. armeniaca</i> and <i>M. pumila</i> ) and forestland (e.g., <i>P. orientalis</i> , <i>P. tabuliformis</i> and <i>R. pseudoacacia</i> )	Loessial Mein soil	Hilly-gully region
Yangjuangou	109.52	36.71	2	535	8.5	1000-1500	65	Cropland (millet and maize), grassland (e.g., <i>S. bungeana</i> ), shrubland (e.g., <i>H. rhamnoides</i> ), orchard (e.g., <i>P. armeniaca</i> and <i>M. pumila</i> ) and forestland (e.g., <i>R. pseudoacacia</i> and <i>P. spp</i> )	Loessial Mein soil	Hilly-gully region

MAP: mean annual precipitation (1961–2020); MAT: mean annual temperature (1961–2020).